Real-Time $\mathcal{L}_1$ Adaptive Control Algorithm in Uncertain Networked Control Systems

Xiaofeng Wang, Evgeny Kharisov, Naira Hovakimyan

Abstract

This paper studies the real-time implementation of output-feedback $\mathcal{L}_1$ adaptive controller over real-time networks. Event-triggering schedules the data transmission dependent upon errors exceeding certain threshold. Continuous-time and discrete-time $\mathcal{L}_1$ adaptive control algorithms are provided. We show that with the proposed event-triggering schemes the states and the input in the networked system can be arbitrarily close to those of a stable reference system by increasing the sampling frequency and the transmission frequency. Stability conditions, in terms of event threshold and allowable transmission delays, are also provided, which can serve as the guidance in real-time scheduling.

I. Introduction

With the progress in digital technology, networked control systems appear in more and more applications, such as power grids, transportation systems, and robotics, to name a few. In such systems, computers are used to compute the control input, and the feedback loops are closed via real-time communication networks. The introduction of digital devices, such as computers and networks, can be advantageous in terms of lower system costs due to streamlined installation and maintenance costs.

There are several challenges in controlling such systems. First challenge comes from the communication network. Communication, especially wireless communication, takes place over a digital network, which means that information is transmitted in discrete time rather than continuous time. Moreover, because all real-time networks have limited bandwidth, the information transmission has to be scheduled in an appropriate manner for a proper operation of the control system.

Second challenge is due to computation limitation of computers. When implementing controllers in a computer, the computation takes place in a discrete-time manner. Therefore, although

Xiaofeng Wang and Naira Hovakimyan are with the Department of Mechanical Science and Engineering, University of Illinois at Urbana-Champaign, Urbana, IL 61801; e-mail: wangx,nhovakim@illinois.edu; Evgeny Kharisov is with the Department of Aerospace Engineering, University of Illinois at Urbana-Champaign, Urbana, IL 61801; e-mail: evgeny@illinois.edu. Research is supported by AFOSR under Contract No.FA9550-09-1-0265.

the plant might be continuous-time, a discrete-time control algorithm is desired. Besides that, timing is also important in implementation, which is especially true when using embedded processors that have very limited computation ability. One needs to know how fast the control inputs must be computed, and when to transmit the inputs to the plant for actuation.

The third challenge is to handle uncertainties and disturbances inside the systems. Physical processes are usually described by reduced order mathematical models under a certain set of simplified assumptions. There is always a mismatch between mathematical models and real plants. Such mismatch may drive the real system behaving far away from the ideal model. Therefore, a robust controller is important to overcome the negative impact of the system uncertainties and exogenous disturbances.

To address these issues, the researchers began to study the impact of communication, computation, and uncertainties on the system performance. Most of the prior work studies only one particular factor without taking care of the rest. However, in practice, these three factors are in fact coupled together: the communication model affects the system robustness w.r.t. the uncertainties; the computation resource determines how aggressive the control algorithm can be; the control algorithm influences the communication model and software architecture, etc. Therefore, the approaches in the prior work might not be desirable in many applications. There is a lack of systematic approaches that address all these issues simultaneously.

This paper provides such an approach. In our approach, one first design the controller without the consideration of the computation and communication constraints; then event-triggered communication scheme is designed and the allowable transmission delays are quantified while still assuming the controller is continuous-time; The third step is to choose appropriate sampling period to discretize the continuous-time controller; finally, one needs to verify the stability conditions of the system under the co-design scheme.

The system under consideration is networked and computer-controlled with nonlinear modeling uncertainties. We use event-triggering technique to trigger data transmissions from the plant/controller to the controller/plant. The data is transmitted when some error signals exceed pre-specified thresholds. A discrete-time output-feedback control algorithm is provided based on the $\mathcal{L}_1$ adaptive control architecture. We derive the performance bounds on the difference between the states and the inputs of the uncertain networked system and a stable reference system, in terms of event threshold, allowable transmission delays, and sampling period in the controller. A stability condition ensuring such boundedness is presented, which describes the tradeoff between the control performance and the communication/comuptation (C&C) parameters. Furthermore, we show that the performance bounds can be made arbitrarily small by improving the quality of C&C, which means that the performance of the uncertain system is subject to the hardware

limitations.

This paper is organized as follows. Section II discusses the prior work. The problem is formulated in Section III. The co-design procedure is presented in Section IV. The communication scheme is developed in Section V and the discrete-time control algorithm is introduced in Section VI. Section VII shows the simulation results. Conclusions are drawn in Section VIII.

II. Prior Work

To the best of our knowledge, this is the first comprehensive result for output-feedback systems that simultaneously addresses the robustness issue as well as the timing issue in C&C. We attempt to answer the following questions:

- How frequently should the data be transmitted over the network and how much transmission delay the system can tolerate?
- How fast should the computation take place?
- How should one design the discrete-time controller that ensures system robustness with respect to uncertainties and disturbances?

Although a lot of prior work has been done to address these problems, most of them only focuses on one of these three questions, which may be impractical in many applications as we mentioned in Section I. In the following discussion, we will go through the existing results and demonstrate their relations to our work.

The traditional approach to address the timing issues in sampled-data systems used periodic task model [1], [2], [3], where consecutive invocations (also called jobs) of a control task are released in a periodic manner. When approaching networked control systems, a positive constant, called the *maximal allowable transfer interval* (MATI), was defined for scheduling the data transmissions over real-time networks [4]. As long as the time interval between two subsequent message transmissions is less than the MATI, asymptotic stability of the close-loop system can be guaranteed [4], [5]. This work was extended to input-to-state stability (ISS) in [6]. All of the work assumes that the computation is continuous. These approaches of estimating task period, however, can be very conservative in a sense that the selected task period is very short. So the control task may have greater utilization than it actually needs. This results in significant over-provisioning of the real-time system hardware, which makes it expensive to provide hard real-time guarantees on message delivery in communication networks.

For this reason, researchers started to consider sporadic task models that can more effectively balance the communication cost against the control performance. A hardware realization of such models is called event-triggering, where the task is executed whenever a pre-specified event occurs [7], [8], [9], [10], [11] and the occurrence of the event can be detected by an event

detector. A software realization of sporadic task models is called self-triggering, where the next task release time is written explicitly as a function of the previously sampled states [12], [13], [14], [15]. This software approach may be appropriate when the hardware implementation is unacceptable. But in general, self-triggering is more conservative than event-triggering, since basically self-triggering conservatively approximates the time instant when an event occurs. Although a lot of work has been done on event/self-triggering, most of them restrict their attention to state-feedback systems, in which case the controller does not have dynamics and therefore the computation frequency is the same as communication frequency. Moreover, the control input, in this case, is actuated whenever the computation task is finished. Therefore there is no need to pay extra attention to the period selection for the computation tasks and the input actuation.

Things are different for output-feedback systems, where the controller may have dynamics. In this case, one needs to schedule two-sided communication: the transmission from the plant to the controller and the transmission of control inputs from the controller to the plant. There is little work on event-triggered output systems. One scheme is provided in [16] for passive systems. However, the controller is still static with linear feedback gain. A more related scheme was proposed in [17] with the assumption that the computation is continuous, namely that the computation constraints are neglected. Moreover, the transmission delays in this work are also assumed to be neglectable and the system dynamics is completely known. Compared with this work, we provide not only the two-sided communication scheme, but also the real-time constraints in computation and bounds on transmission delays that ensures stability of the uncertain output-feedback system. Although we adopt $\mathcal{L}_1$ adaptive control architecture, our approach to address the C&C issues is applicable to any control structures.

Another related research field is the area of adaptive control, which handles the system uncertainties through control adaptation based on feedback of signals in a control system. Traditional model reference adaptive control (MRAC) studies stable performance without the consideration of the system's input/output performance during the transient phase [18]. The system uncertainties during the transient however may lead to unpredictable/undesirebale situations such as generating large transient errors and control signals with high-frequency and/or large amplitudes, or slow the convergence of the tracking errors. As a result, application of these approaches is limited. Improvement of the transient performance of adaptive controllers has been addressed in [19], [20], [21], [22], to name a few. All bounds in this work, however, are only for tracking errors. Uniform performance in system inputs and outputs are not taken into account, which may lead to high-gain feedback. These issues have been addressed using $\mathcal{L}_1$ adaptive control [23] recently. One thing worth mentioning is that all of this prior work assumes signals in control systems are all continuous. For networked systems with limited C&C resources, these approaches may

drive the entire systems unstable. With this concern in mind, we study the impact of C&C on the adaptive control architectures and provide appropriate scheme to deal with C&C issues.

III. Problem Formulation

Notations: We denote by $\mathbb{N}$ the set of natural numbers, by $\mathbb{R}^n$ the n-dimensional real vector space, and by $\mathbb{R}^+$ the set of the real positive numbers. Let $\mathbb{R}_0^+ = \mathbb{R}^+ \cup \{0\}$. We use $\|\cdot\|$ to denote the Euclidean norm of a vector and the induced 2-norm of a matrix. The maximal and minimal singular values of a matrix P are denoted by $\lambda_{\max}(P)$ and $\lambda_{\min}(P)$, respectively. $\|\cdot\|_{\mathcal{L}_1}$ and $\|\cdot\|_{\mathcal{L}_\infty}$ are the $\mathcal{L}_1$ norm and the $\mathcal{L}_\infty$ norm of a function, respectively. The truncated $\mathcal{L}_\infty$ norm of a function $x : \mathbb{R}_0^+ \to \mathbb{R}^n$ is defined as $\|x\|_{\mathcal{L}_\infty^{[0,\tau]}} = \sup_{0\le t\le\tau} \|x(t)\|$. The symbol e is used for exponential function to distinguish it from the tracking error e. The Laplace transform of a function $x(t)$ is denoted by $x(s) = \mathfrak{L}[x(t)]$. The inverse Laplace transform of $x(s)$ is denoted as $x(t) = \mathfrak{L}^{-1}[x(s)]$. Given $c \in \mathbb{R}_0^+$, $\lfloor c \rfloor$ is the largest integer that is less than or equal to c. For a function of time $x(t)$, sometimes we drop the argument t and use just x for brevity.

Consider an output-feedback Multi-Input-Multi-Output (MIMO) system:

$$\begin{aligned} \dot{x}(t) &= Ax(t) + B(u(t) + g(t, x)), \\ y(t) &= Cx(t), \quad x(0) = x_0, \end{aligned} \tag{1}$$

where $x : \mathbb{R}_0^+ \to \mathbb{R}^n$ is the state, $u : \mathbb{R}_0^+ \to \mathbb{R}^m$ is the control input, $y : \mathbb{R}_0^+ \to \mathbb{R}^l$ is the system output, $A \in \mathbb{R}^{n\times n}$, $B \in \mathbb{R}^{n\times m}$, $C \in \mathbb{R}^{l\times n}$ are known and $g : \mathbb{R}_0^+ \times \mathbb{R}^n \to \mathbb{R}^m$ is an unknown function. We assume that (A, B) is controllable and (A, C) is observable. Also assume that B has full column rank m, and the row rank of C is greater than or equal to m. As to the unknown function g, we have the following assumption:

Assumption 3.1: Function $g(t, x)$ is locally Lipschitz w.r.t. x and bounded at $x = 0$, uniformly in t, i.e. given a positive constant $\rho \in \mathbb{R}^+$, there exist positive constants $L_\rho^g, \rho_0 \in \mathbb{R}^+$, such that

$$\|g(t, x_1) - g(t, x_2)\| \le L_\rho^g \|x_1 - x_2\| \quad \text{and} \quad \|g(t, 0)\| \le \rho_0$$

hold for any $t \ge 0$ and any $x_1, x_2 \in \{x \in \mathbb{R}^n \mid \|x\| \le \rho\}$. Assume that given ρ, L_ρ^g is known.

In our framework, the control inputs are computed by a centralized computer and the information is exchanged between the plant and the controller over a real-time network. Notice that the data transmission from the plant/controller to the controller/plant cannot be continuous due to the limited channel capacity. Therefore, one has to determine when to transmit the data. Four monotonic sequences are used to characterize the transmission release time instants and finishing time instants:

- $s_r[i] \in \mathbb{R}_0^+$ is the time instant when the i^{th} transmission from the plant to the controller (called "plant transmission") is released;

- $s_f[i] \in \mathbb{R}_0^+$ is the time instant when the data in the i^{th} transmission from the plant to the controller is ready to be used by controller;
- $\tau_r[i] \in \mathbb{R}_0^+$ is the time instant when the i^{th} transmission from the controller to the plant (called "control transmission") is released;
- $\tau_f[i] \in \mathbb{R}_0^+$ is the time instant when the input data in the i^{th} transmission from the controller to the plant is actuated.

We use $T_{\text{P}}[i] = s_r[i+1] - s_r[i]$ and $T_{\text{C}}[i] = \tau_r[i+1] - \tau_r[i]$ to denote the i^{th} inter-transmission intervals in the plant and control transmissions, respectively. The i^{th} delays in the plant and control transmissions are denoted by $\Delta_{\text{P}}[i] = s_f[i] - s_r[i]$ and $\Delta_{\text{C}}[i] = \tau_f[i] - \tau_r[i]$, respectively. Let $\bar{\Delta}_{\text{P}} = \sup_{i\in\mathbb{N}} \Delta_{\text{P}}[i]$ and $\bar{\Delta}_{\text{C}} = \sup_{i\in\mathbb{N}} \Delta_{\text{C}}[i]$.

The controller receives the packet from the plant at $s_f[i]$. We use $y_{\text{C}}(t)$ to denote the controller's latest information on the system output. Note that $y_{\text{C}}(t)$ is piecewise constant since $y_{\text{C}}(t) = y(s_r[i])$ for any $t \in [s_f[i], s_f[i+1])$. The received information is used to compute the virtual control input $u_{\text{C}}(kT_s)$, $k = 0, 1, \cdots$ with a sampling period T_s, according to a discrete-time control algorithm. Again, due to the limited communication resource, not all $u_{\text{C}}(kT_s)$ are transmitted to the plant and actuated. Instead, only a subsequence of $\{u_{\text{C}}(kT_s)\}_{k=0}^{\infty}$ is transmitted. Therefore the actual control input $u(t)$ is also piecewise constant, where

$$u(t) = u_{\text{C}}(\tau_r[i]), \quad \forall t \in [\tau_f[i], \tau_f[i+1]). \tag{2}$$

Notice that the control transmission release time $\tau_r[i]$ is in fact a multiple of T_s.

The objective is to co-design the real-time control algorithm and the communication protocols that drive the real system to follow an ideal model, in the presence of uncertain nonlinearity, disturbances, and communication/ computation constraints, where the ideal model is defined by

$$\begin{aligned} \dot{x}_{\text{id}}(t) &= A_m x_{\text{id}}(t) + B k_g r(t), \\ y_{\text{id}}(t) &= C x_{\text{id}}(t), \\ x_{\text{id}}(0) &= \hat{x}_0. \end{aligned} \tag{3}$$

In the equations above, $x_{\text{id}} : \mathbb{R}_0^+ \to \mathbb{R}^n$ is the ideal state, $r : \mathbb{R}_0^+ \to \mathbb{R}^l$ is the bounded tracking signal with $r_{\max} = \|r\|_{\mathcal{L}_\infty}$, and $\hat{x}_0 \in \mathbb{R}^n$ is the known ideal initial condition satisfying $C\hat{x}_0 = Cx_0$. We assume that $r(t)$ is piecewise constant with the sampling period T_s. Also assume that there exist a $K \in \mathbb{R}^{m\times n}$ such that $A_m = A + BK$ is Hurwitz, which means there must exist two positive-definite symmetric matrices $P \in \mathbb{R}^{n\times n}$ and $Q \in \mathbb{R}^{n\times n}$ such that

$$PA_m + A_m^\top P = -Q. \tag{4}$$

The system in (1) can be equivalently rewritten as

$$\begin{aligned} \dot{x}(t) &= A_m x(t) + B(u(t) + f(t,x)), \\ y(t) &= Cx(t), \quad x(0) = x_0, \end{aligned} \tag{5}$$

where $f(t,x) = g(t,x) - Kx$ satisfies, according to Assumption 3.1,

$$\|f(t,x_1) - f(t,x_2)\| \leq L_\rho \|x_1 - x_2\|, \tag{6}$$

$$\|f(t,0)\| \leq \rho_0, \tag{7}$$

for any $t \geq 0$ and any $x_1, x_2 \in \{x \in \mathbb{R}^n \mid \|x\| \leq \rho\}$, where $L_\rho = L_\rho^g + \|K\|$. Therefore, the original problem, which focuses on the difference between system (1) and the ideal model, is equivalent to the problem that studies the difference between the ideal model and the system in (5), where $f(t,x)$ is treated as the uncertainty.

IV. Co-Design Procedure

To implement a discrete-time controller for a continuous-time plant, we need not only the control algorithm itself, but also timing constraints that ensure the control inputs are actuated at the right moment. This paper uses so-called "emulation-based" method [6] to co-design the discrete-time control algorithm and the associated real-time constraints. The basic idea unfolds in the following three steps:

1) Establish a control algorithm without the consideration of the computation and communication constraints;
2) Develop communication scheme, but still assuming the controller is continuous-time;
3) Choose appropriate sampling period to discretize the continuous-time controller.

Remark 4.1: The first step basically seeks continuous-time controller for the plant. This is a traditional controller design problem in a classic control theory. Although we do provide an output-feedback adaptive control architecture, it is not the main emphasis of this paper. We pay more attention to the other two steps, which studies the impact of communication/computation constraints on the system performance. In the second step, besides the communication protocols, we also need to derive the stability condition, including quantifying the maximal allowable inter-transmission intervals and the maximal allowable transmission delays, with which the system stability can be preserved. These two parameters are also important for the selection of sampling period in the third step. Basically the sampling period must be smaller than the inter-transmission intervals. Finally, once the discretization of the controller is done, we need to go back and verify the stability condition obtained in the second step.

Although this paper focuses on adaptive controllers, this is a general procedure to discretize controllers for continuous-time plants in a real-time manner. It applies for different stability concepts. The specific stability concept that this paper considers is the closeness between the real system in (5) and the ideal model in (3). In other words, we try to provide uniform performance bounds between the signals in these two systems. To fulfill this objective, we introduce an intermediate system, called "reference system", as a bridge between the real system and the ideal model:

$$\begin{aligned} \dot{x}_{\rm ref}(t) &= A_m x_{\rm ref}(t) + B(u_{\rm ref} + f(t, x_{\rm ref})), \\ y_{\rm ref}(t) &= C x_{\rm ref}(t), \quad x_{\rm ref}(0) = \hat{x}_0, \\ u_{\rm ref}(s) &= -F(s)\sigma_{\rm ref}(s) + F(s)k_g r(s), \end{aligned} \tag{8}$$

where $F(s)$ is a low-pass filter and $\sigma_{\rm ref}(s)$ is the Laplace Transform of $f(t, x_{\rm ref}(t))$. Let

$$H(s) = (s\mathbb{I} - A_m)^{-1}, \tag{9}$$

$$G(s) = H(s)B(1 - F(s)). \tag{10}$$

The stability of the reference system is established by the following lemma:

Lemma 4.1 ([23]): Consider the reference system in (8). For any $F(s)$ and $\rho_{x_{\rm ref}} \in \mathbb{R}_0^+$ satisfying $\|\hat{x}_0\| < \rho_{x_{\rm ref}}$, and

$$\|G(s)\|_{\mathcal{L}_1} < \frac{\rho_{x_{\rm ref}} - \|H(s)BF(s)k_g\|_{\mathcal{L}_1} r_{\max} - \|H(s)\hat{x}_0\|_{\mathcal{L}_\infty}}{\rho_{x_{\rm ref}} L_{\rho_{x_{\rm ref}}} + \rho_0},$$

the inequalities $\|x_{\rm ref}\|_{\mathcal{L}_\infty} < \rho_{x_{\rm ref}}$ and $\|u_{\rm ref}\|_{\mathcal{L}_\infty} < \rho_{u_{\rm ref}}$ hold, where

$$\rho_{u_{\rm ref}} = \|F(s)\|_{\mathcal{L}_1}(\rho_{x_{\rm ref}} L_{\rho_{x_{\rm ref}}} + \rho_0) + \|F(s)k_g\|_{\mathcal{L}_1} r_{\max}.$$

The relation between this reference system and the ideal system in (3) has been established in the following lemma:

Lemma 4.2 ([23]): Assume that the hypotheses in Lemma 4.1 hold. Then $\|x_{\rm id} - x_{\rm ref}\|_{\mathcal{L}_\infty} \leq \|G(s)\|_{\mathcal{L}_1}\rho_{x_{\rm ref}}$ holds and $\|G(s)\|_{\mathcal{L}_1} \to 0$ as the bandwidth of $F(s)$ goes to $+\infty$. Moreover, there exist a positive constant ρ_e such that $\|u_{\rm id} - u_{\rm ref}\|_{\mathcal{L}_\infty} \leq \rho_e$ holds and ρ_e decreases as the bandwidth of $F(s)$ increases

With these results, in order to study the closeness between the real system and the ideal model, we only need to consider the difference between the real system and the reference system.

V. Communication Constraints with Continuous-time Controller

This section discusses the real-time constraints on the communication. We adopt $\mathcal{L}_1$ adaptive controller that is assumed to be continuous-time, namely that we do not consider the computation

constraints in this section. Therefore, in this section, the virtual control input (the control input computed by the controller, but not necessarily transmitted and actuated) is also continuous. To distinguish it from the virtual control input of the discrete-time control algorithm $u_{\rm C}(kT_s)$, we denote the continuous-time virtual control input by $v_{\rm C}(t)$. In the following discussion, we will introduce the $\mathcal{L}_1$ adaptive control architecture, the event-triggered data transmission schemes, and the related stability analysis.

A. Continuous-Time $\mathcal{L}_1$ Adaptive Controller

An $\mathcal{L}_1$ adaptive controller consists of three components: state predictor, adaptation law, and low-pass filter. The state predictor is defined by

$$\begin{aligned} \dot{\hat{x}}(t) &= A_m\hat{x}(t) + B\hat{v}_{\rm C}(t) + \hat{\sigma}(t), \\ \hat{y}(t) &= C\hat{x}(t), \quad \hat{x}(0) = \hat{x}_0, \end{aligned} \tag{11}$$

where $\hat{\sigma}(t)$ is the estimate of the uncertainty and

$$\hat{v}_{\rm C}(t) = v_{\rm C}(\tau_r[i]), \quad \forall t \in [\tau_r[i], \tau_r[i+1]). \tag{12}$$

Notice that $\hat{v}_{\rm C}(t)$ is in fact a sampled version of $v_{\rm C}(t)$. $v_{\rm C}(\tau_r[i])$ is the data released by the controller for the control transmission. The difference between $\hat{v}_{\rm C}(t)$ and $u(t)$ is that the actual control input $u(t)$ is a "delayed" version of $\hat{v}_{\rm C}(t)$ as follows:

$$u(t) = v_{\rm C}(\tau_r[i]), \quad \forall t \in [\tau_f[i], \tau_f[i+1]), \tag{13}$$

where the delays are due to the communication limitations. Let

$$\Lambda = \begin{pmatrix} C^\top & (D\sqrt{P})^\top \end{pmatrix}^\top, \tag{14}$$

where $D \in \mathbb{R}^{n-l\times n}$ ensures $D(C\sqrt{P}^{-1})^\top = 0$ and Λ invertible. We define

$$A_o = \Lambda A_m \Lambda^{-1}. \tag{15}$$

The estimate of the uncertainty, $\hat{\sigma}(t)$, is updated according to the piecewise adaptation law:

$$\hat{\sigma}(t) = \Phi(T_s) \begin{pmatrix} y_{\rm C}(kT_s) - \hat{y}(kT_s) \\ 0 \end{pmatrix} \tag{16}$$

for any $t \in [kT_s, (k+1)T_s)$, where

$$\Phi(T_s) = \left(\int_0^{T_s} {\rm e}^{A_o(T_s-\tau)}\Lambda d\tau \right)^{-1} e^{A_oT_s}. \tag{17}$$

Recall that $y_{\rm C}(t)$ is the latest output that the controller has received from the plant at time t. For all $t \in [s_f[i], s_f[i+1])$, $y_{\rm C}(t)$ is constant. The virtual control input

$$v_{\rm C}(s) \;=\; -W(s)\hat{\sigma}(s) + F(s)k_g r(s), \tag{18}$$

where

$$W(s) \;=\; F(s)H_c(s)^{-1}\hat{C}CH(s), \tag{19}$$

$$H_c(s) \;=\; \hat{C}CH(s)B, \tag{20}$$

$H(s)$ is defined in (9), $F(s)$ is a low-pass filter with relative degree $d_F > d_{H_c} - d_H$, d_{H_c} and d_H are the relative degrees of $H_c(s)$ and $\hat{C}CH(s)$, respectively, and $\hat{C} \in \mathbb{R}^{m\times l}$ is an arbitrary matrix that ensures $H_c(s)$ invertible and minimal phase. The existence of $\hat{C}$ is guaranteed by the assumption that B has full column rank m and m is less than or equal to the row rank of C. Such selection of $F(s)$ and $\hat{C}$ ensures that $W(s)$ is also a proper and stable lower-pass filter.

Remark 5.1: This is a typical $\mathcal{L}_1$ adaptive control architecture, which has high-frequency estimation and low-frequency control. The main challenge of analyzing the system performance lies in the mismatch in the signals (u, $\hat{v}_{\rm C}$, $v_{\rm C}$) and (y, $y_{\rm C}$), due to the communication constraints.

B. Event-Triggered Data Transmission

In order to determine the release time instants $s_r[i]$ and $\tau_r[i]$, we use event-triggering technique. Two event detectors are located at the plant and the controller. At the plant, the event detector continuously monitors the output $y(t)$ and checks a pre-specified logic rule $E_{\rm P}$. The release of the $i+1^{\rm st}$ plant transmission is triggered when $E_{\rm P}$ is false, where

$$E_{\rm P} : \|y(t) - y(s_r[i])\| \leq \epsilon_{\rm s} \tag{21}$$

and $\epsilon_{\rm s}$ is a positive constant. Mathematically, we have

$$s_r[i+1] = \min_{t>s_r[i]} \{t \in \mathbb{R}_0^+ \mid \|y(t) - y(s_r[i])\| \geq \epsilon_{\rm s}\}.$$

At the moment $s_r[i]$, the data $y(s_r[i])$ is transmitted and at time $s_f[i]$ the controller can use this data. Consequently, $y_{\rm C}(t) = y(s_r[i])$ for any $t \in [s_f[i], s_f[i+1])$.

Similarly, there is an event detector at the controller to monitor $v_{\rm C}(t)$. The release of the $i+1^{\rm st}$ control transmission is triggered when $E_{\rm C}$ becomes false, where

$$E_{\rm C} : \|v_{\rm C}(t) - v_{\rm C}(\tau_r[i])\| \leq \epsilon_{\rm u} \tag{22}$$

and $\epsilon_{\rm u}$ is a positive constant. Mathematically, we have

$$\tau_r[i+1] = \min_{t>\tau_r[i]} \{t \in \mathbb{R}_0^+ \mid \|v_{\rm C}(t) - v_{\rm C}(\tau_r[i])\| \geq \epsilon_{\rm u}\}.$$

In this case, we know $u(t) = v_{\rm C}(\tau_r[i])$ for any $t \in [\tau_f[i], \tau_f[i+1])$. The overall system structure is shown in Figure 1.

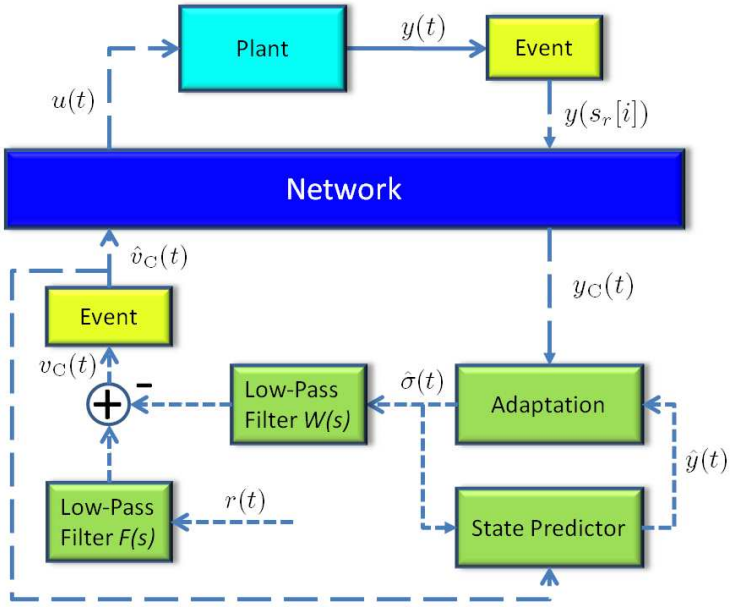

Fig. 1: $\mathcal{L}_1$ adaptive control architecture in a networked control system

C. Stability Analysis

This subsection studies the stability of the close-loop system with the proposed control algorithm and the event-triggering communication scheme. We derive bounds on $\|x - x_{\rm ref}\|_{\mathcal{L}_\infty}$ and $\|u - u_{\rm ref}\|_{\mathcal{L}_\infty}$. The analysis can be split into four steps:

1) Assuming that $\|x\|_{\mathcal{L}_\infty^{[0,t^*]}}$ and $\|u\|_{\mathcal{L}_\infty^{[0,t^*]}}$ are bounded, find the bound on $\|y_{\rm C}(t) - y(t)\|$, which is the error due to communication limitation (Lemma 5.1);
2) With the bound on $\|y_{\rm C}(t) - y(t)\|$, derive the bound on the estimate error $\|y(t) - \hat{y}(t)\|$ (Lemma 5.2);
3) With the bounds on $\|y(t) - \hat{y}(t)\|$, derive the bound on $\|x_{\rm ref} - x\|_{\mathcal{L}_\infty^{[0,t^*]}}$, while still assuming that $\|x\|_{\mathcal{L}_\infty^{[0,t^*]}}$ and $\|u\|_{\mathcal{L}_\infty^{[0,t^*]}}$ are bounded (Lemma 5.3);
4) Relax the assumption of the boundedness of $\|x\|_{\mathcal{L}_\infty^{[0,t^*]}}$ and $\|u\|_{\mathcal{L}_\infty^{[0,t^*]}}$ (Theorem 5.4).

Lemma 5.1: Consider the system (5) with the controller in (11)–(18) and the event-triggering scheme in (21) and (22). Given $t^* \geq 0$, if there exist ρ_x, $\rho_u \in \mathbb{R}^+$ such that $\|x(t)\| \leq \rho_x$ and $\|u(t)\| \leq \rho_u$ hold for any $t \in [0, t^*)$, then

$$\|y_{\rm C}(t) - y(t)\| \quad \leq \quad \epsilon_{\rm s} + \phi(\rho_x, \rho_u)\bar{\Delta}_{\rm P} \tag{23}$$

holds for any $t \in [0, t^*)$, where $\phi : \mathbb{R}^+ \times \mathbb{R}^+ \to \mathbb{R}^+$ is defined by

$$\phi(\rho_x, \rho_u) = \|CA_m\|\rho_x + \|CB\|\rho_u + \|C\|(L_{\rho_x}\rho_x + \rho_0), \tag{24}$$

$\bar{\Delta}_{\rm P}$ is the upper bound on the delays in plant transmissions, and L_{ρ_x} is the Lipschitz constant of $f(t,x)$ over the compact set $\{x \in \mathbb{R}^n \mid \|x\| \le \rho_x\}$.

Remark 5.2: The function $\phi(\rho_x, \rho_u)$ in (24) is an upper bound on the growth rate of $\|y_{\rm C}(t) - y(t)\|$. The term $\phi(\rho_x, \rho_u)\bar{\Delta}_{\rm P}$ quantifies the impact of delays on the error $\|y_{\rm C}(t) - y(t)\|$.

Let us now consider the second step. We first need to introduce some functions and parameters. Let $\eta_1 : \mathbb{R}_0^+ \to \mathbb{R}^{l\times l}$, $\eta_2 : \mathbb{R}_0^+ \to \mathbb{R}^{l\times n-l}$, $\eta_3 : \mathbb{R}_0^+ \to \mathbb{R}^{l\times m}$, $\eta_4 : \mathbb{R}_0^+ \to \mathbb{R}^{l\times n}$ be defined by

$$[\eta_1^\top(T_s), \eta_2^\top(T_s)] = (\mathbb{I}_{l\times l}, 0_{l\times n-l})e^{A_o T_s}, \tag{25}$$

$$\eta_3(T_s) = (\mathbb{I}_{l\times l}, 0_{l\times n-l}) \int_0^{T_s} e^{A_o(T_s-\tau)}\Lambda B d\tau, \tag{26}$$

$$\eta_4(T_s) = (\mathbb{I}_{l\times l}, 0_{l\times n-l}) \int_0^{T_s} e^{A_o(T_s-\tau)} d\tau \Phi(T_s), \quad \text{and} \tag{27}$$

$$\beta_i(T_s) = \|\eta_i(T_s)\|, \quad i = 1,2,3,4, \tag{28}$$

where A_o is defined in (15). Note that $\lim_{T_s\to 0}\beta_i(T_s) = 0$ holds for $i = 2, 3$ and $\beta_1(T_s)$, $\beta_4(T_s)$ converge to a constant when $T_s \to 0$, [23].

Given $\rho_x \in \mathbb{R}_0^+$, we define

$$\theta(T_s, \epsilon_{\rm u}, \mu) = (\beta_1(T_s) + \beta_4(T_s) + 1)\varsigma(T_s, \epsilon_{\rm u}, \mu) - \beta_1(T_s)\mu + \beta_4(T_s)\mu, \tag{29}$$

where

$$\varsigma(T_s, \epsilon_{\rm u}, \mu) = \beta_1(T_s)\mu + \beta_2(T_s)\sqrt{\frac{\alpha}{\lambda_{\min}(P_o)}} + \beta_3(T_s)(\epsilon_{\rm u} + \sigma_{\max}), \tag{30}$$

$$\sigma_{\max} = L_{\rho_x}\rho_x + \rho_0, \tag{31}$$

$$\alpha = \max\left\{\lambda_{\max}(P_o)\left(\frac{2(\|P_o\Lambda B\|\epsilon_{\rm u} + \|P_o\Lambda B\|\sigma_{\max})}{\lambda_{\min}(Q_o)}\right)^2, \tilde{x}_0^\top P\tilde{x}_0\right\}, \tag{32}$$

$$P_o = (\Lambda^{-1})^\top P\Lambda^{-1}, \quad Q_o = (\Lambda^{-1})^\top Q\Lambda^{-1}, \tag{33}$$

Λ is defined in (14), and $\tilde{x}_0 = x_0 - \hat{x}_0$. As shown in the following lemma, the term $\theta(T_s, \epsilon_{\rm u}, \mu)$ in fact is the bound on the error $\|y(t) - \hat{y}(t)\|$, which goes to zero as $T_s, \epsilon_{\rm u}, \mu$ go to zero.

Lemma 5.2: Consider the system (5) with the controller in (11)–(18) and the event-triggering scheme in (21) and (22). Given $t^* \ge 0$, assume that there exists $\rho_x \in \mathbb{R}^+$ such that $\|x(t)\| \le \rho_x$ holds for any $t \in [0, t^*)$. If

$$\exists \mu \in \mathbb{R}^+, \text{ s.t. } \|y(t) - y_{\rm C}(t)\| \le \mu, \quad \text{and} \tag{34}$$

$$\|\hat{v}_{\rm C}(t) - u(t)\| \le \epsilon_{\rm u}, \tag{35}$$

for any $t \in [0, t^*)$, where $\hat{v}_{\rm C}(t)$ is defined in (12), then

$$\|y(t) - \hat{y}(t)\| \le \theta(T_s, \epsilon_{\rm u}, \mu), \quad \forall t \in [0, t^*), \tag{36}$$

$$\|y_{\rm C}(kT_s) - \hat{y}(kT_s)\| \le \mu + \varsigma(T_s, \epsilon_{\rm u}, \mu), \quad k = 0, 1, \cdots, \left\lfloor \frac{t^*}{T_s} \right\rfloor. \tag{37}$$

With the bounds in Lemma 5.2, we can bound the error $\|x(t) - x_{\rm ref}(t)\|$.

Lemma 5.3: Assume that the hypotheses in Lemma 5.2 hold and

$$1 - \|G(s)\|_{\mathcal{L}_1} L_{\rho_x} > 0. \tag{38}$$

Then

$$\|x(t) - x_{\rm ref}(t)\| \leq \frac{b_1\theta(T_s, \epsilon_{\rm u}, \mu) + (b_2 + b_4)\epsilon_u + b_3}{1 - \|G(s)\|_{\mathcal{L}_1} L_{\rho_x}}$$

holds for any $t \in [0, t^*)$, where

$$\begin{aligned} b_1 &= \|H(s)BF(s)H_c(s)^{-1}\hat{C}\|_{\mathcal{L}_1}, \quad b_2 = \|H(s)BF(s)\|_{\mathcal{L}_1}, \\ b_3 &= \left\|H(s) - H(s)BF(s)H_c(s)^{-1}\hat{C}CH(s)\right\|_{\mathcal{L}_1} \rho_{\tilde{x}_0}, \quad b_4 = 2\|H(s)B\|_{\mathcal{L}_1}, \end{aligned} \tag{39}$$

$\rho_{\tilde{x}_0}$ is the bound on $\|\tilde{x}_0\|$, and $H(s)$, $G(s)$, $H_c(s)$ are defined in (9), (10), (20), respectively. Furthermore, the inequality

$$\|F(s)\sigma(s) - W(s)\hat{\sigma}(s)\|_{\mathcal{L}_\infty^{[0,t^*]}} \leq b_5\theta(T_s, \epsilon_{\rm u}, \mu) + b_6 + \|F(s)\|_{\mathcal{L}_1}\epsilon_{\rm u} \tag{40}$$

holds, where

$$b_5 = \|F(s)H_c(s)^{-1}\hat{C}\|_{\mathcal{L}_1} \quad \text{and} \quad b_6 = \|F(s)H_c(s)^{-1}\hat{C}CH(s)\|_{\mathcal{L}_1}\rho_{\tilde{x}_0}.$$

Theorem 5.4: Consider the system (5) with the controller in (11)–(18) and the event-triggering scheme in (21) and (22). Assume that the inequality

$$\Delta_{\rm C}[i] \leq T_{\rm C}[i], \quad \forall i \in \mathbb{N} \tag{41}$$

holds. If $\bar{\Delta}_{\rm P}$, $\epsilon_{\rm s}$, $\epsilon_{\rm u}$, T_s, $F(s)$ are chosen in a way such that there exist $\gamma_x, \gamma_u \in \mathbb{R}^+$ satisfying inequality (38),

$$\frac{b_1\theta(T_s, \epsilon_{\rm u}, \mu) + (b_2 + b_4)\epsilon_{\rm u} + b_3}{1 - \|G(s)\|_{\mathcal{L}_1} L_{\rho_x}} < \gamma_x, \quad \text{and} \tag{42}$$

$$\|F(s)\|_{\mathcal{L}_1} L_{\rho_x}\gamma_x + b_5\theta(T_s, \epsilon_{\rm u}, \mu) + b_6 + \|F(s)\|_{\mathcal{L}_1}\epsilon_{\rm u} < \gamma_u \tag{43}$$

where

$$\mu = \bar{\Delta}_{\rm P}\phi(\rho_x, \rho_u) + \epsilon_{\rm s}, \tag{44}$$

$$\rho_x = \rho_{x_{\rm ref}} + \gamma_x \tag{45}$$

$$\rho_u = \rho_{u_{\rm ref}} + \gamma_u \tag{46}$$

and $\phi(\rho_x, \rho_u)$ is defined in (24), with the initial conditions satisfying $\|x(0) - x_{\rm ref}(0)\| < \gamma_x$ and $\|v_{\rm C}(0) - u_{\rm ref}(0)\| < \gamma_u$, then $\|x - x_{\rm ref}\|_{\mathcal{L}_\infty} \leq \gamma_x$ and $\|v_{\rm C} - u_{\rm ref}\|_{\mathcal{L}_\infty} \leq \gamma_u$ hold. Moreover, inequality (37) holds for any $k = 0, 1, \cdots, +\infty$.

Remark 5.3: Notice that inequality (41) implies $\tau_r[i] \leq \tau_f[i] \leq \tau_r[i+1]$. It means that when the controller releases the $i+1^{\text{st}}$ transmission of the data $v_{\text{C}}(\tau_r[i+1])$, the plant at least receives the ith packet with the data $v_{\text{C}}(\tau_r[i])$. Therefore, by the event-triggering condition in (22) and the definitions of $u(t)$ and $\hat{v}_{\text{C}}(t)$ in (2) and (12), we know that for any $t \geq 0$, the inequality $\|\hat{v}_{\text{C}}(t) - u(t)\| \leq \epsilon_{\text{u}}$ holds. To be more precise, $\|\hat{v}_{\text{C}}(t) - u(t)\| = \epsilon_u$ for any $t \in [\tau_r[i], \tau_f[i])$ and $\|\hat{v}_{\text{C}}(t) - u(t)\| = 0$ for any $t \in [\tau_f[i], \tau_r[i+1])$.

Remark 5.4: Though the $\mathcal{L}_1$ conditions in (42) and (43) seem complicated, we can always tune the parameters to ensure the existence of γ_x and γ_u. It can be stated as follows: for any γ_x and γ_u satisfying $\frac{b_3}{1-\|G(s)\|_{\mathcal{L}_1} L_{\rho x}} < \gamma_x$ and $b_6 < \gamma_u$, there always exist positive constants ω^*, ϵ_{s}^*, ϵ_{u}^*, Δ_{P}^*, and T^* such that for any tuple $(\omega, \epsilon_{\text{s}}, \epsilon_u, T_s, \bar{\Delta}_{\text{P}})$ satisfying $\omega \geq \omega^*$, $\epsilon_{\text{s}} \leq \epsilon_{\text{s}}^*$, $\epsilon_u \leq \epsilon_u^*$, $\bar{\Delta}_{\text{P}} \leq \Delta_{\text{P}}^*$, and $T_s \leq T^*$, the stability conditions in (42) and (43) hold, where the parameter ω is the bandwidth of the low-pass filter $F(s)$. We will further discuss the relationship between these parameters in the next section.

Theorem 5.4 provides sufficient conditions in (42) and (43) to ensure the stability of the close-loop system. However, the bound on the delays in the control transmission, $\bar{\Delta}_{\text{C}}$, is not involved in these conditions. It does not mean that $\bar{\Delta}_{\text{C}}$ can be arbitrarily large. In fact, an implicit bound is placed on $\bar{\Delta}_{\text{C}}$, which is inequality (41). It is easy to see that if we can derive a lower bound on $T_{\text{C}}[i]$ and enforce $\bar{\Delta}_{\text{C}}$ to be less than this lower bound, then inequality (41) will hold. With this idea, we can have an explicit expression on the allowable $\bar{\Delta}_{\text{C}}$. The lower bound on $T_{\text{C}}[i]$ is given in the following corollary.

Corollary 5.5: Assume that the hypotheses in Theorem 5.4 hold. Then the inter-transmission intervals $T_{\text{P}}[i]$ and $T_{\text{C}}[i]$ satisfy

$$T_{\text{C}}[i] \geq \frac{\epsilon_{\text{u}}}{\psi(\delta, T_s)} \quad \text{and} \quad T_{\text{P}}[i] \geq \frac{\epsilon_{\text{s}}}{\phi(\rho_x, \rho_u)} \tag{47}$$

for $i = 0, 1, \cdots, +\infty$, where $\psi : \mathbb{R}_0^+ \times \mathbb{R}_0^+ \to \mathbb{R}_0^+$ is defined by

$$\psi(\delta, T_s) = \delta(\|H_W(s)\Phi(T_s)\|_{\mathcal{L}_1} + \|C_W B_W \Phi(T_s)\|) + (\|H_F(s)\|_{\mathcal{L}_1} + \|C_F B_F k_g\|)\, r_{\max} \tag{48}$$

$$\delta = \mu + \varsigma(T_s, \epsilon_{\text{u}}, \mu), \tag{49}$$

$$H_W(s) = C_W A_W (s\mathbb{I} - A_W)^{-1} B_W, \tag{50}$$

$$H_F(s) = C_F A_F (s\mathbb{I} - A_F)^{-1} B_F k_g, \tag{51}$$

$\Phi(T_s)$, ϕ, ρ_x, ρ_u, μ are defined in (17), (24), (48), (45), (46), (44), respectively, and (A_W, B_W, C_W), (A_F, B_F, C_F) are the state-space realizations of $W(s)$, $F(s)$, respectively.

With Corollary 5.5, we can see that if the transmission delays satisfy

$$\Delta_{\text{C}}[i] \leq \bar{\Delta}_{\text{C}} = \frac{\epsilon_{\text{u}}}{\psi(\delta, T_s)}, \tag{52}$$

then inequality (41) can be enforced and therefore we obtain a computable bound on the delays in control transmissions. The function $\psi(\delta, T_s)$, in fact, is an upper bound on the growth rate of the error $\|v_{\rm C}(t) - v_{\rm C}(\tau_i[i])\|$, which will be used later for the analysis of the discrete-time control algorithm.

D. Example

This subsection provides a simple example to show how to verify the stability conditions in (42), (43), and (52). Consider a single-input-single-output system:

$$\dot{x} = \underbrace{\begin{bmatrix} 0 & 1 \\ -1 & -1.4 \end{bmatrix}}_{A_m} x + \underbrace{\begin{bmatrix} 0 \\ 1 \end{bmatrix}}_{B}(u + f(t,x)), \quad y = \underbrace{[1 \;\; 0]}_{C} x, \quad x(0) = [0 \;\; 0]^\top$$

with the uncertainty $f(t,x) = 0.9x_1 + 0.7x_2 + 0.07x_2^2 + 0.1x_3^2 - 0.1\cos x_1$. With $\rho_{x_{\rm ref}} = 1.6$, we can verify the Lipschitz constant of $f(t, x_{\rm ref})$ is 1.62 and $\rho_0 = 0.1$. The low-pass filter is chosen to be $F(s) = \frac{40^2}{s^2+32s+40^2}\left(\frac{40}{s+40}\right)^2$ and the tracking gain is $k_g = 1$. With the tracking signal $r(t) = 1$, the condition in Lemma 4.1 can be verified, which means that the reference system (8) is stable.

We now seek the allowable event thresholds ($\epsilon_{\rm s}$ and $\epsilon_{\rm u}$), transmission delays ($\bar{\Delta}_{\rm P}$ and $\bar{\Delta}_{\rm C}$), and the adaptation period (T_s) to verify the conditions in Theorem 5.4. Let $\gamma_x = 0.5$ and $\gamma_u = 5$. Then $\rho_x = 2.1$ according to (45) and $L_\rho = 1.72$. With $\epsilon_{\rm s} = 10^{-3}$, $\epsilon_{\rm u} = 10^{-2}$, $\bar{\Delta}_{\rm P} = 10^{-4}$, and $T_s = 2.5 \times 10^{-4}$, the $\mathcal{L}_1$ stability conditions in (42) and (43) can be satisfied. Under this setting, we compute $\psi(\delta, T_s) = 10^3$, which implies $\bar{\Delta}_{\rm C} = 10^{-5}$ according to (52).

Remark 5.5: The stability conditions in (42), (43) indicate a simple tradeoff relation between the parameters $\epsilon_{\rm s}$, $\epsilon_{\rm u}$, $\bar{\Delta}_{\rm P}$, and T_s. Inequality (52) shows that $\bar{\Delta}_{\rm C}$ is mainly determined by ϵ_u and T_s. Note that large $\epsilon_{\rm u}$ results in small T_s according to the previously mentioned tradeoff, which leads to large $\Phi(T_s)$ and therefore large $\psi(\delta, T_s)$. So large $\epsilon_{\rm u}$ will not only provide a large nominator in $\frac{\epsilon_{\rm u}}{\psi(\delta, T_s)}$, but also leads to a large denominator, which brings out an optimization problem of choosing maximal allowable $\bar{\Delta}_{\rm C}$. The impact of the bandwidth of the low-pass filter on the other parameters might is not obvious in (42) and (43). It will not only affect the parameters b_i, but also the denominator $1 - \|G(s)\|_{\mathcal{L}_1} L_{\rho_x}$ in the left side of (42). In the example, the simulation results show that the smaller the bandwidth is, the larger the other parameters are, as long as the bandwidth can ensure the stability of the reference system. Further work will be done to study the relation between parameters.

VI. Discrete-Time Control Algorithm

This section studies how to discretize the continuous-time controller proposed in the previous section. We take advantage of the fact that the plant only needs the value of $v_{\rm C}(t)$ at the

moment of releasing control transmission, i.e. $v_{\rm C}(\tau_r[i])$. The value of $v_{\rm C}(t)$ over the time interval $(\tau_r[i], \tau_r[i+1])$ is not necessary for the plant at all. This enables us to discretize the controller. In fact, the virtual control input of the discrete-time control algorithm, $u_{\rm C}(kT_s)$, is the sampled data of $v_{\rm C}(t)$.

One important thing is that during discretization, we need to ensure that the $\mathcal{L}_1$ stability conditions in (42) and (43) still hold. Note that in this case, $s_f[i]$ and $\tau_r[i]$ are multiples of T_s, since the controller uses the newly received data and releases the control input to the network only at the time instants that are multiples of T_s. Let $s_f[i] = k_i^s T_s$ and $\tau_r[i] = k_i^\tau T_s$.

A. Discrete-Time $\mathcal{L}_1$ Adaptive Controller

Discretizing the $\mathcal{L}_1$ adaptive controller in (11) - (18) with the sampling period T_s, the state predictor is then

$$\begin{aligned} \hat{x}((k+1)T_s) &= \hat{A}_m \hat{x}(kT_s) + \hat{B}_1 \hat{u}_{\rm C}(kT_s) + \hat{B}_2 \hat{\sigma}(kT_s) \\ \hat{y}(kT_s) &= C\hat{x}(kT_s), \quad \hat{x}(0) = C\hat{x}_0 \end{aligned}$$

where

$$\hat{A}_m = e^{A_m T_s}, \quad \hat{B}_2 = \int_0^{T_s} e^{A_m(T_s - s)} ds, \quad \hat{B}_1 = \hat{B}_2 B, \tag{53}$$

and $\hat{u}_{\rm C}(kT_s) = u_{\rm C}(k_i^\tau T_s) = u_{\rm C}(\tau_r[i])$ for any $k \in \mathbb{N}$ satisfying $kT_s \in [\tau_r[i], \tau_r[i+1])$, i.e. $k = k_i^\tau, \cdots, k_{i+1}^\tau - 1$. The estimate of the uncertainty, $\hat{\sigma}(kT_s)$, is still updated according to the piecewise adaptation law in (16).

Recall that (A_W, B_W, C_W) and (A_F, B_F, C_F) are the state-space realizations of $W(s)$ and $F(s)$, respectively. With the state space realizations of $W(s)$ and $F(s)$, we can discretize the filters with the sampling period T_s. The virtual control input is composed of two parts: one part is associated with the state of $W(s)$, $x_W(kT_s)$, and the other part is associated with the state of $F(s)$, $x_F(kT_s)$. It is computed in the following way:

$$\begin{aligned} x_W((k+1)T_s) &= \hat{A}_W x_W(kT_s) + \hat{B}_W \hat{\sigma}(kT_s), \quad x_W(0) = 0, \\ x_F((k+1)T_s) &= \hat{A}_F x_F(kT_s) + \hat{B}_F k_g r(kT_s), \quad x_F(0) = 0, \\ u_{\rm C}(kT_s) &= -C_W x_W(kT_s) + C_F x_F(kT_s), \end{aligned} \tag{54}$$

where

$$\begin{aligned} \hat{A}_W = C_W e^{A_W T_s}, \quad \hat{B}_W = C_W \int_0^{T_s} e^{A_W(T_s - s)} B_W ds, \\ \hat{A}_F = C_F e^{A_F T_s}, \quad \hat{B}_F = C_F \int_0^{T_s} e^{A_F(T_s - s)} B_F ds. \end{aligned}$$

B. Communication Scheme

Similar to Subsection V-B, the release of the $i+1^{\text{st}}$ plant transmission is triggered when the logic E_{P}^{d} is false, where

$$E_{\text{P}}^{\text{d}} : \|y(t) - y(s_r[i])\| \leq \epsilon_{\text{s}}. \tag{55}$$

The event at the controller side is different since the virtual control input is not continuous any more. In this case, the release of the $i+1^{\text{st}}$ control transmission is triggered when the logic E_{C}^{d} becomes false, where

$$E_{\text{C}}^{\text{d}} : \|u_{\text{C}}(kT_s) - u_{\text{C}}(\tau_r[i])\| \leq \epsilon_{\text{u}}^{\text{d}} \tag{56}$$

and $\epsilon_{\text{u}}^{\text{d}}$ is a positive constant to be determined. Still, $u(t) = u_{\text{C}}(k_i^\tau T_s) = u_{\text{C}}(\tau_r[i])$ for any $t \in [\tau_f[i], \tau_f[i+1])$. Note that in this case, when the control transmission is released, we cannot conclude $\|u_{\text{C}}(\tau_r[i+1]) - u_{\text{C}}(\tau_r[i])\| = \epsilon_{\text{u}}^{\text{d}}$ any more. In fact, $\|u_{\text{C}}(\tau_r[i+1]) - u_{\text{C}}(\tau_r[i])\| \geq \epsilon_{\text{u}}^{\text{d}}$. But we know

$$\|u_{\text{C}}(\tau_r[i+1] - T_s) - u_{\text{C}}(\tau_r[i])\| \leq \epsilon_{\text{u}}^{\text{d}}\,, \tag{57}$$

since at time instant $\tau_r[i+1] - T_s$, the logic E_{C}^{d} is still not violated.

C. Stability Analysis

The analysis is similar to that in Subsection V-C. The challenge lies in the boundedness of $\|u_{\text{C}}(kT_s) - u_{\text{C}}(\tau_r[i])\|$. Since $\tau_r[i] = k_i^\tau T_s$, we know that for any integer $k \in [k_i^\tau, k_{i+1}^\tau - 1]$, inequality (56) holds and

$$\begin{aligned} & \|u_{\text{C}}(\tau_r[i+1]) - u_{\text{C}}(\tau_r[i])\| \\ \leq\ & \|u_{\text{C}}(k_{i+1}^\tau T_s) - u_{\text{C}}((k_{i+1}^\tau - 1)T_s)\| + \|u_{\text{C}}((k_{i+1}^\tau - 1)T_s) - u_{\text{C}}(\tau_r[i])\| \\ \leq\ & \|u_{\text{C}}(k_{i+1}^\tau T_s) - u_{\text{C}}((k_{i+1}^\tau - 1)T_s)\| + \epsilon_{\text{u}}^{\text{d}}. \end{aligned} \tag{58}$$

Therefore, in order to bound $\|u_{\text{C}}(\tau_r[i+1]) - u_{\text{C}}(\tau_r[i])\|$, we need to study $\|u_{\text{C}}(k_{i+1}^\tau T_s) - u_{\text{C}}((k_{i+1}^\tau - 1)T_s)\|$. Note that in the continuous-time case, the growth rate of $v_{\text{C}}(t)$ is bounded by $\psi(\delta, T_s)$, as shown in Corollary 5.5, with δ defined in (49). Since the discrete-time controller imitates the continuous-time controller, we have

$$\|u_{\text{C}}(k_{i+1}^\tau T_s) - u_{\text{C}}((k_{i+1}^\tau - 1)T_s)\| \leq \psi(\delta, T_s)T_s. \tag{59}$$

Let

$$\epsilon_{\text{u}} = \epsilon_{\text{u}}^{\text{d}} + \psi(\delta, T_s)T_s. \tag{60}$$

Then, with inequalities (58) and (59), we have

$$\|u_{\rm C}(\tau_r[i+1]) - u_{\rm C}(\tau_r[i])\| \leq \epsilon_{\rm u}.$$

We can then present the stability conditions for the discrete-time version:

Theorem 6.1: Consider the system (5) with the controller in (54) and the event-triggering scheme in (55) and (56). If $\bar{\Delta}_{\rm P}$, $\epsilon_{\rm s}$, $\epsilon_{\rm u}^{\rm d}$, T_s, $F(s)$ are chosen in a way such that there exist $\gamma_x, \gamma_u \in \mathbb{R}^+$ satisfying the $\mathcal{L}_1$ stability conditions in (42) and (43) with $\epsilon_{\rm u}$ defined in (60), the delays in control transmissions satisfy

$$\Delta_{\rm C}[i] \leq \bar{\Delta}_{\rm C} = \frac{\epsilon_{\rm u}^{\rm d}}{\psi(\delta, T_s)}, \quad \forall i \in \mathbb{N}, \tag{61}$$

and the initial conditions satisfy $\|x(0) - x_{\rm ref}(0)\| < \gamma_x$ and $\|u_{\rm C}(0) - u_{\rm ref}(0)\| < \gamma_u$, then $\|x - x_{\rm ref}\|_{\mathcal{L}_\infty} \leq \gamma_x$ and $\|u_{\rm C}(kT_s) - u_{\rm ref}(kT_s)\| \leq \gamma_u$ for all $k \in \mathbb{N}$.

Proof: The idea is to construct the signal between $u_{\rm C}(kT_s)$ and $u_{\rm C}((k+1)T_s)$, say $u_{\rm C}(t)$ for all $t \in (kT_s, (k+1)T_s)$, such that $u_{\rm C}(t)$ becomes continuous and follows $v_{\rm C}(t)$ in (18). Then we can apply Theorem 5.4 to draw the conclusion. Due to the space limitation, we omit the detailed proof. ■

Remark 6.1: The stability conditions in (42), (43), and (61) show that small $\epsilon_{\rm s}$, $\epsilon_{\rm u}^{\rm d}$, $\bar{\Delta}_{\rm P}$, $\bar{\Delta}_{\rm C}$, T_s admit small γ_x and γ_u. Moreover, γ_x and γ_u go to zero if these parameters reduce to zero. This result suggests that the more powerful communication and computation are, the better control performance we can achieve, which means that the control performance is subject to the hardware limitation.

D. Real-Time Computation

This subsection discusses how the discrete-time control algorithm runs in a real-time manner. The basic idea is shown in Figure 2. Let us start from the control transmission release time $\tau_r[i]$, which is a multiple of T_s, say $\tau_r[i] = kT_s$. The black block represents that the computation of one iteration is being executed. The empty block represents that the logic rule in (56) is being checked.

The iteration from k to $k+1$, which is the computation of $u_{\rm C}((k+1)T_s)$, and the examination of the event $E_{\rm C}^{\rm d}$ must be finished within T_s unit-time since $\tau_r[i]$. The next iteration starts after $(k+1)T_s$, but not necessary to be exactly at $(k+1)T_s$. As long as the iteration and the event examination are completed before $(k+2)T_s$, it is fine. Assume that during the iteration from $k+1$ to $k+2$, a new packet is received from the plant, for example at $t_1 \in ((k+1)T_s, (k+2)T_s)$. This reception will not affect the current iteration (from $k+1$ to $k+2$) and the event examination. This packet will be used in the next iteration, which is from $k+2$ to $k+3$. That is why $s_f[i]$

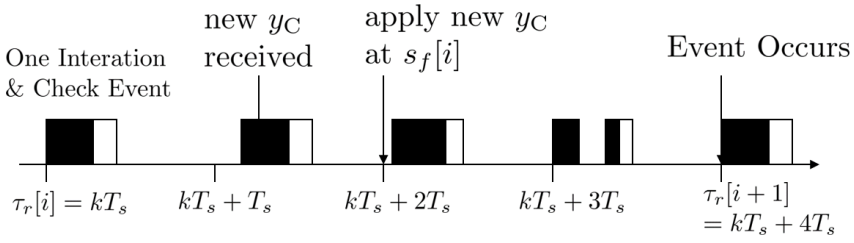

Fig. 2: The computation history at the controller

is always a multiple of T_s for the discrete-time case, as we mentioned in context. During this process, if $E_{\mathrm{C}}^{\mathrm{d}}$ becomes false, then data transmission happens and $\tau_r[i+1]$ is defined.

VII. Simulations

For the simulation example we consider the model of a two-link robot arm from [24]. The robotic arm consists of two links and two joints as it is shown in Figure 3. Both angles α and θ as well as angular velocities ω_1 and ω_2 are measurable. The measurements are sent to the controller over the communication network. Each joint has a build-in actuator, which receives the commands independently over the network.

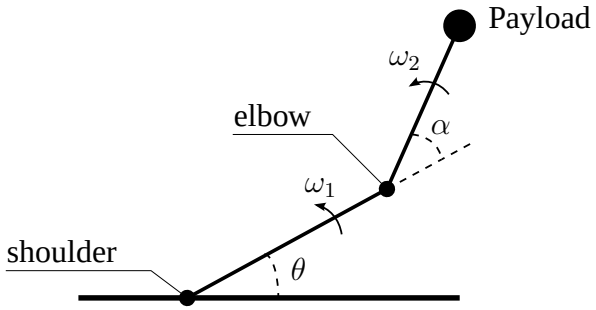

Fig. 3: Two-link robot arm scheme.

The dynamics equations of the robotic arm [24] are given by

$$\dot{\alpha}(t) = \omega_2(t) - \omega_1(t)\,, \tag{62}$$

$$\dot{\theta}(t) = \omega_1(t)\,, \tag{63}$$

$$\begin{bmatrix} \dot{\omega}_1(t) \\ \dot{\omega}_2(t) \end{bmatrix} = F(\alpha(t)) \begin{bmatrix} \omega_1^2(t) \\ \dot{\omega}_2^2(t) \end{bmatrix} + G(\alpha(t)) \begin{bmatrix} Q_1(t) \\ Q_2(t) \end{bmatrix}\,, \tag{64}$$

where

$$F(\alpha(t)) = \frac{J_{12}\sin\alpha(t)}{\Delta(\alpha(t))}\begin{bmatrix} J_{12}\cos\alpha(t) & J_{22} \\ -J_{11} & -J_{12}\cos\alpha(t) \end{bmatrix},$$

$$G(\alpha(t)) = \frac{1}{\Delta(\alpha(t))}\begin{bmatrix} J_{22} & -J_{22}-J_{12}\cos\alpha(t) \\ -J_{12}\cos\alpha(t) & J_{11}+J_{12}\cos\alpha(t) \end{bmatrix},$$

$$\Delta(\alpha(t)) = J_{11}J_{22} - J_{12}^2\cos^2\alpha(t)\,,$$

and $Q_1(t)$, $Q_2(t)$ are the moments at the joints; J_{11}, J_{12}, J_{22} are the moments of inertia, which are not precisely known. The moments acting at the joints are given by

$$Q_1(t) = u_1(t) + T_{v1}(t) + \sigma_1(t)\,,$$
$$Q_2(t) = u_2(t) + T_{v2}(t) + \sigma_2(t)\,,$$

where $T_{v1}(t) = -v_1\omega_1(t)$ and $T_{v2}(t) = v_2(\omega_1(t) - \omega_2(t))$ are the moments due to viscous friction with v_1, v_2 being the unknown viscous friction coefficients; $\sigma_1(t)$, $\sigma_2(t)$ are the external disturbances; and $u_1(t)$, $u_2(t)$ are the control torques generated by the actuators.

For the simulations we consider three scenarios:

S1. Let the moment of inertia be given by $J_{11} = 7/3$, $J_{12} = 3/2$, $J_{22} = 4/3$, and the viscous friction coefficients be given by $v_1 = 1$, $v_2 = 0.5$. In this scenario we consider the system without external disturbance, that is $\sigma_1(t) \equiv \sigma_2(t) \equiv 0$.

S2. Let $J_{11} = 2$, $J_{12} = 1$, $J_{22} = 2$, and $v_1 = 1.3$, $v_2 = 0.7$. Also assume $\sigma_1(t) \equiv \sigma_2(t) \equiv 0$.

S3. Consider the same $J_{11} = 2$, $J_{12} = 1$, $J_{22} = 2$, $v_1 = 1.3$, v_2 =0.7 but let the disturbance be given by $\sigma_1(t) = 1 + 0.2\cos(0.1t)$, $\sigma_2(t) = -0.7\sin(10t)$.

The first two scenarios consider different parametric uncertainties, and the third scenario considers system input periodic disturbance with two harmonics of different amplitude. We use the same $\mathcal{L}_1$ controller for these three scenarios without re-tuning the controller parameters . This will help us to examine some properties of our control algorithm such as uniform transient performance and disturbance attenuation, which verify our theoretical results.

We start the design of the $\mathcal{L}_1$ adaptive controller with linearization of the system dynamics (62)-(64) about the initial condition $x_0 = [0.1 \quad 0 \quad -0.3 \quad 0]^\top$. The linearized system matrixes are given by

$$A = \begin{bmatrix} 0 & 1 & 0 & -1 \\ -1.336 & -2.165 & 0 & 3.854 \\ 0 & 0 & 0 & 1 \\ 1.024 & 1.599 & 0 & -3.108 \end{bmatrix},\ B = \begin{bmatrix} 0 & 0 \\ -1.689 & 4.330 \\ 0 & 0 \\ 1.509 & -3.198 \end{bmatrix},\ C = \begin{bmatrix} 1 & 0 & 0 & 0 \\ 0 & 0 & 1 & 0 \end{bmatrix}.$$

The eigenvalues of A are $\lambda_1 = 0$, $\lambda_2 = -4.6584$, $\lambda_3 = -0.1256$, $\lambda_4 = -0.4894$. For the design we keep same B and C matrices, and we choose the following A_m:

$$A_m = \begin{bmatrix} 0 & 1 & 0 & 0 \\ -1 & -2 & 0 & 0 \\ 0 & 0 & 0 & 1 \\ 0 & 0 & -1 & -2 \end{bmatrix},$$

which has the desired location of the system poles. For the implementation of the discrete-time $\mathcal{L}_1$ adaptive controller we compute $\hat{A}_m$, $\hat{B}_1$ and $\hat{B}_2$ according to (53). For the control law, we choose a third order lowpass filter of the form

$$F(s) = \frac{\omega_{c1}^2}{s^2 + 2\omega_{c1}\zeta s + \omega_{c1}^2} \frac{\omega_{c2}}{s + \omega_{c2}},$$

where $\omega_{c1} = 10$, $\zeta = 1.2$, $\omega_{c2} = 15$. The sampling time of the $\mathcal{L}_1$ adaptation law is set to $T_s = 0.0005$ s. The event thresholds for the control signal is chosen to be $\epsilon_{\rm u} = 0.01$ and for the plant output $\epsilon_{\rm s} = 0.001$. The time delays in plant/control transmissions are assumed to be random for each packet and bounded by $\bar{\Delta}_{\rm P} = \bar{\Delta}_{\rm C} = 0.003$ s.

Figure 4 shows the response of the closed-loop system with discrete-time $\mathcal{L}_1$ adaptive controller for Scenario 1 to the step reference command $r = [0.5 \quad 0.5]^\top$. We see that the response of the $\mathcal{L}_1$ adaptive controller almost coincide with the response of the $\mathcal{L}_1$ reference system, which has transient specifications similar to the ideal system. The effect of the system uncertainty is compensated within the bandwidth of the lowpass filter. From the closeness of the $\mathcal{L}_1$ adaptive control system and the reference system we see that the communication network does not significantly affect the closed-loop system performance.

The simulation results for the second and the third scenarios are shown in Figure 5, and 6 respectively. We see that system preserves similar transient performance in the case of severe changes of uncertainties without any retuning of the controller. Response of the closed-loop system in Figure 6 shows that the adaptive controller attempts to compensate for the frequency range of the disturbance within the bandwidth of the lowpass filter.

Figure 7 shows the system responses for the step input signals with different size. All simulations are performed for Scenario 1. From the figure we see that the closed-loop system has uniform predictable transient response for different step input commands.

Finally, we consider the continuous time implementation of the $\mathcal{L}_1$ adaptive controller. For verification of the theoretical claims we use the same settings as for the simulations of the discrete time $\mathcal{L}_1$ adaptive controller in Figure 4. The simulation results for the continuous-time adaptive controller in Figure 8 show identical performance to the discrete-time case.

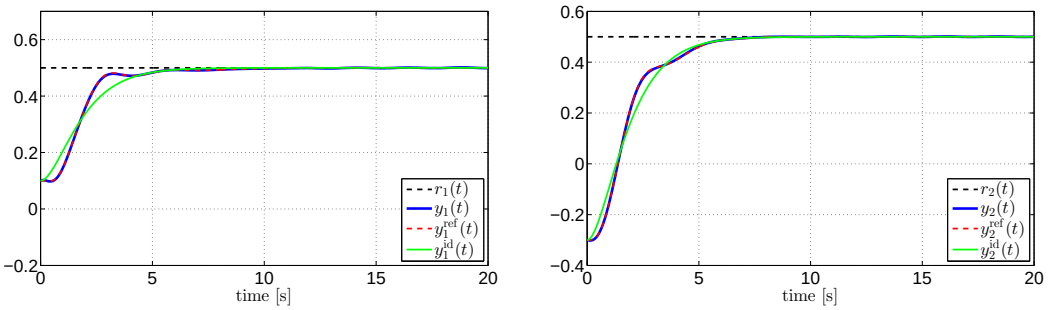

(a) Response of the first system output

(b) Response of the second system output

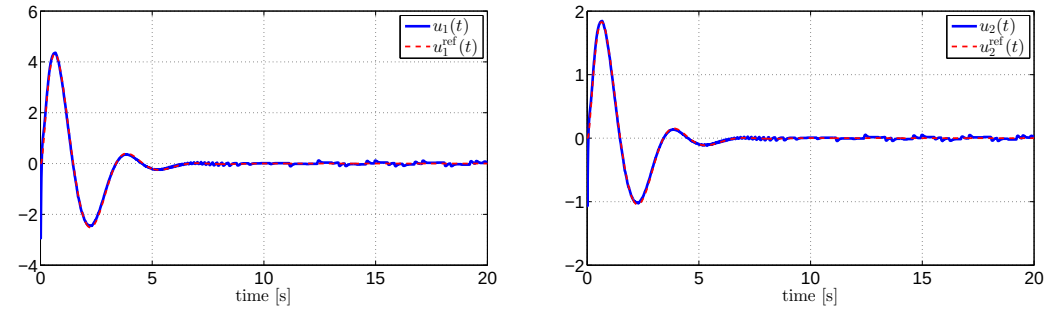

(c) First control input history

(d) Second control input history

Fig. 4: Step response of the closed-loop system with $\mathcal{L}_1$ adaptive controller, $\mathcal{L}_1$ reference system, and the ideal system for Scenario 1. The response of the $\mathcal{L}_1$ adaptive controller almost coincide with the response of the $\mathcal{L}_1$ reference system, which has transient specifications similar to the ideal system.

VIII. Conclusions

This paper studies real-time implementation of $\mathcal{L}_1$ adaptive controller over networks using event-triggered data transmission. Continuous-time and discrete-time control algorithms are provided. The proposed schemes ensure that the signals in the real system can be arbitrarily close to those of a stable reference system by increasing the sampling frequency and the transmission frequency. We provide real-time constraints for stability. Efficient management of C&C resource to meet these constraints will be addressed in future papers.

IX. Proofs

A. Proof of Lemma 5.1

Without the loss of generality, assume that $t^* \in [s_f[k^*], s_f[k^*+1])$. We can divide the interval $[0, t^*)$ into finite number of subintervals $[s_f[k^*], t^*)$ and $[s_f[i], s_f[i+1])$ for $i = 0, 1, \cdots, k^*-1$.

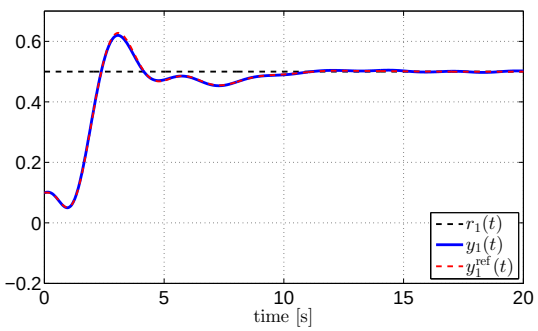

(a) Response of the first system output

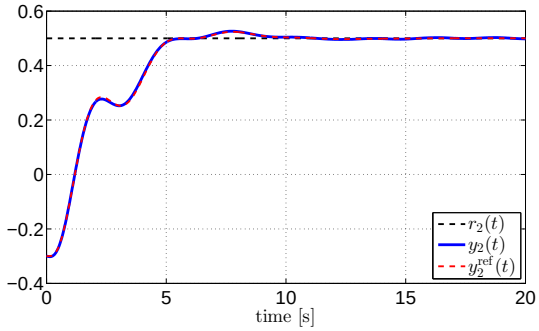

(b) Response of the second system output

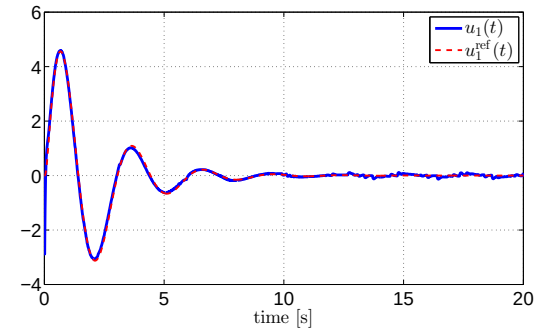

(c) First control input history

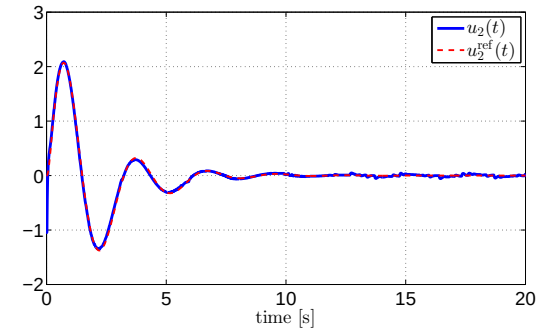

(d) Second control input history

Fig. 5: Step response of the closed-loop system with $\mathcal{L}_1$ adaptive controller and $\mathcal{L}_1$ reference system for Scenario 2. The transient behavior of the closed-loop system is similar to Figure 4.

Based on the event in (21), we know that $\|y(t)-y(s_r[i])\| \leq \epsilon_{\rm s}$ holds for any $t \in [s_r[i], s_r[i+1])$. We now consider $\|y(t)-y(s_r[i])\|$ over $t \in [s_r[i+1], s_f[i+1])$. By (5), we have

$$\begin{aligned}
\frac{d}{dt}\|y(t)-y(s_r[i])\| &\leq \left\|\frac{d}{dt}(y(t)-y(s_r[i]))\right\| \\
&= \|\dot{y}(t)\| = \|CA_m x(t) + CBu(t) + Cf(t,x)\| \\
&\leq \|CA_m\|\|x(t)\| + \|CB\|\|u(t)\| + \|C\|\|f(t,x)\| \\
&\leq \|CA_m\|\rho_x + \|CB\|\rho_u + \|C\|(L_{\rho_x}\rho_x + \rho_0) \\
&= \phi(\rho_x,\rho_u).
\end{aligned}$$

Solving this inequality over $t \in [s_r[i+1], s_f[i+1])$ yields

$$\begin{aligned}
\|y(t)-y(s_r[i])\| &\leq \|y(s_r[i+1])-y(s_r[i])\| + \phi(\rho_x,\rho_u)(t-s_r[i+1]) \\
&\leq \epsilon_{\rm s} + \phi(\rho_x,\rho_u)\bar{\Delta}_{\rm P},
\end{aligned}$$

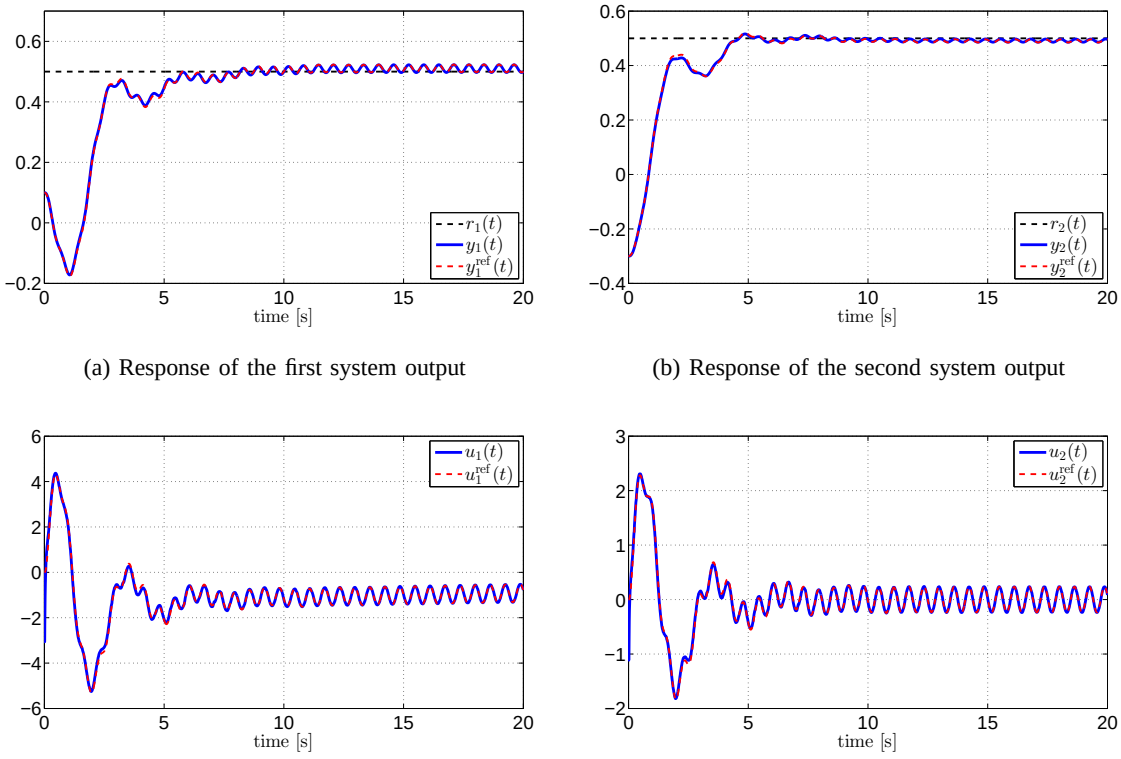

(a) Response of the first system output

(b) Response of the second system output

(c) First control input history

(d) Second control input history

Fig. 6: Step response of the closed-loop system with $\mathcal{L}_1$ adaptive controller and $\mathcal{L}_1$ reference system for Scenario 3. The $\mathcal{L}_1$ adaptive controller compensates for the input disturbance within the lowpass filter bandwidth.

where the second inequality comes from (21). Combining this with (21) yields

$$\|y(t) - y(s_r[i])\| \leq \epsilon_{\rm s} + \phi(\rho_x, \rho_u)\bar{\Delta}_{\rm P}$$

for any $t \in [s_f[i], s_f[i+1]) \subseteq [s_r[i], s_f[i+1])$. The same bound can be obtained for $\|y(t) - y(s_r[k^*])\|$ for any $t \in [s_f[k^*], t^*)$. Note that $y_{\rm C}(t) = y(s_r[i])$ for any $t \in [s_f[i], s_f[i+1])$, with which the preceding inequality implies the satisfaction of (23). ■

B. Proof of Lemma 5.2

We focus on the time interval $[0, t^*)$. Consider the real system and the predictor

$$\begin{aligned} \dot{x}(t) &= A_m x(t) + B(u(t) + f(t,x)), \\ \dot{\hat{x}}(t) &= A_m \hat{x}(t) + B\hat{v}_{\rm C}(t) + \hat{\sigma}(t). \end{aligned}$$

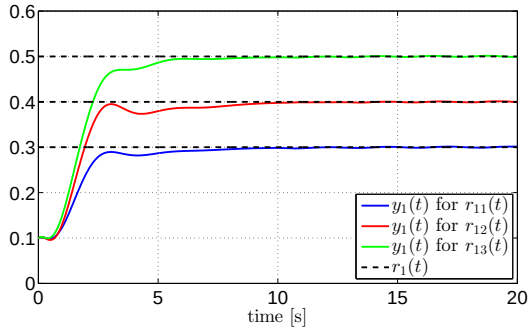

(a) Response of the first system output

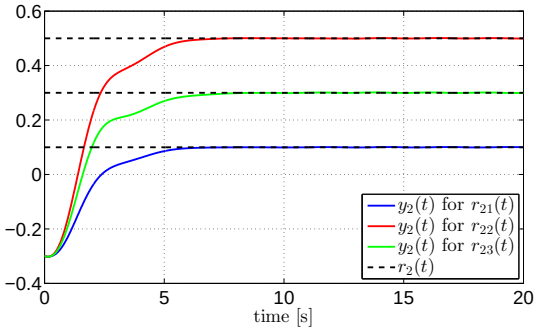

(b) Response of the second system output

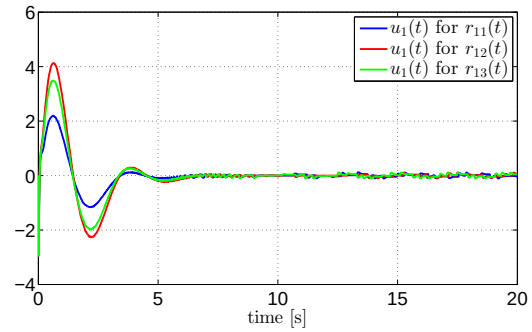

(c) First control input history

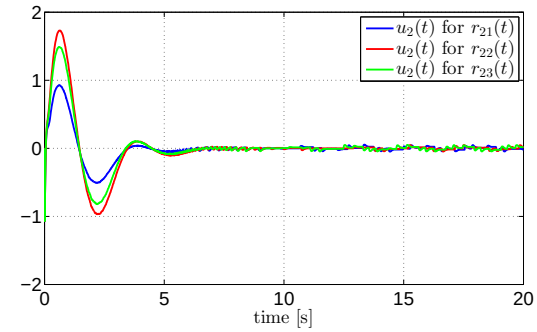

(d) Second control input history

Fig. 7: Transient response of the closed-loop system with $\mathcal{L}_1$ adaptive controller for step commands with different size. The simulations are performed for Scenario 1. The closed-loop system shows uniform predictable performance.

Let $\tilde{x} = x - \hat{x}$, $\tilde{u} = u - \hat{v}_{\rm C}$, and $\tilde{y} = C\tilde{x}$. Then

$$\dot{\tilde{x}}(t) \;=\; A_m\tilde{x}(t) + B\tilde{u}(t) + B\sigma(t) - \hat{\sigma}(t),$$

where $\sigma(t) = f(t, x(t))$. Let $\tilde{\xi} = \Lambda\tilde{x}$. Then

$$\begin{aligned}\dot{\tilde{\xi}}(t) &= A_o\tilde{\xi}(t) + \Lambda B\tilde{u}(t) + \Lambda(B\sigma(t) - \hat{\sigma}(t)),\\ \tilde{\xi}(0) &= \begin{pmatrix} 0 \\ \tilde{y}_\perp(0)\end{pmatrix},\end{aligned}$$

where $\tilde{y}_\perp(0) = D\sqrt{P}\tilde{x}_0$. Recall that $A_o = \Lambda A_m\Lambda^{-1}$, $PA_m + A_m^\top P = -Q$ and $\Lambda = \begin{pmatrix} C^\top, \left(D\sqrt{P}\right)^\top \end{pmatrix}^\top$, where $D(C\sqrt{P}^{-1})^\top = 0$.

In the following discussion, we try to find the upper bounds on $\tilde{\xi}(kT_s)$ and $\tilde{y}(kT_s) = (\mathbb{I}_{l\times l}, 0_{l\times n-l})\tilde{\xi}(kT_s)$. To simplify the notation, sometimes we use $(\mathbb{I}, 0)$ for $(\mathbb{I}_{l\times l}, 0_{l\times n-l})$ if it is

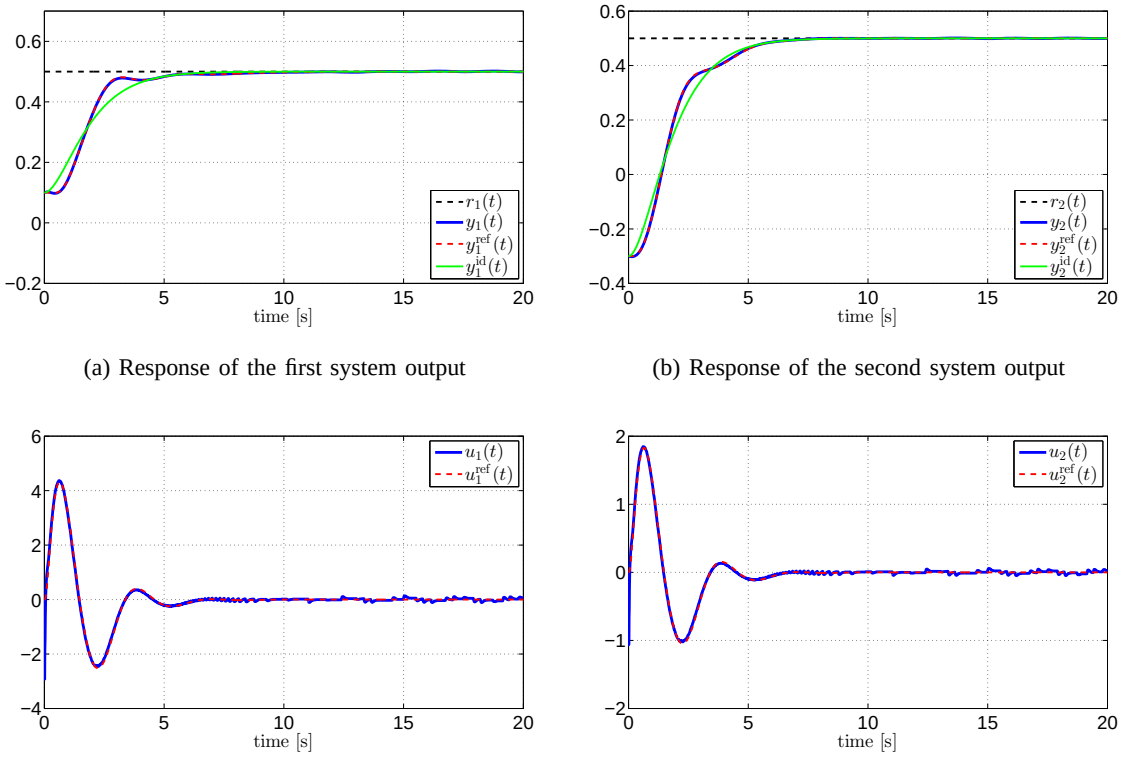

(a) Response of the first system output

(b) Response of the second system output

(c) First control input history

(d) Second control input history

Fig. 8: Simulation results for continuous time $\mathcal{L}_1$ adaptive controller for Scenario 1. The performance of the continuous time $\mathcal{L}_1$ adaptive controller is identical to the results in Figure 4.

clear in context.

We divide the interval $[0, t^*)$ into finite number of subintervals $[k^*T_s, t^*)$ and $[kT_s, (k+1)T_s)$, $k = 0, 1, \cdots, k^* - 1$, where $k^* = \left\lfloor \frac{t^*}{T_s} \right\rfloor$. Consider $\tilde{\xi}(t)$ over $t \in [kT_s, (k+1)T_s)$. We can split $\tilde{\xi}$ into two terms

$$\tilde{\xi}(t) = \chi(t) + \zeta(t),$$

where χ, ζ satisfy

$$\dot{\chi}(t) = A_o\chi(t) - \Lambda\hat{\sigma}(t), \qquad \chi(kT_s) = \begin{pmatrix} y_{\text{C}}(kT_s) - \hat{y}(kT_s) \\ 0 \end{pmatrix},$$

$$\dot{\zeta}(t) = A_o\zeta(t) + \Lambda B\tilde{u}(t) + \Lambda B\sigma(t), \qquad \zeta(kT_s) = \begin{pmatrix} y(kT_s) - y_{\text{C}}(kT_s) \\ \tilde{y}_\perp(kT_s) \end{pmatrix},$$

respectively, and $\tilde{y}_\perp(kT_s) = (0_{n-l\times l}, \mathbb{I}_{n-l\times n-l})\tilde{\xi}(kT_s)$.

We first consider $\chi(t)$. It is easy to see that for any $t \in [kT_s, (k+1)T_s)$

$$\chi(t) \;=\; e^{A_o(t-kT_s)} \begin{pmatrix} y_{\rm C}(kT_s) - \hat{y}(kT_s) \\ 0 \end{pmatrix} - \int_{kT_s}^{t} e^{A_o(t-\tau)} \Lambda \hat{\sigma}(kT_s) d\tau.$$

With the adaptation law in (16), we have

$$\chi((k+1)T_s) \;=\; 0. \tag{65}$$

We now consider $\zeta(t)$ over $t \in [kT_s, (k+1)T_s)$. Let $V(\zeta) = \zeta^\top P_o \zeta$. We use mathematical induction to show that for any $k \in \{0, \cdots, k^* - 1\}$,

$$\begin{aligned} \|\tilde{y}(kT_s)\| &\le \varsigma(T_s, \epsilon_{\rm u}, \mu), \\ V(\zeta(kT_s)) &\le \alpha = \max\left\{ \lambda_{\max}(P_o) \left(\frac{a}{\lambda_{\min}(Q_o)} \right)^2, \tilde{x}_0^\top P \tilde{x}_0 \right\} \end{aligned}$$

hold, where ς is defined in (30) and $a = 2(\|P_o \Lambda B\| \epsilon_{\rm u} + \|P_o \Lambda B\| \sigma_{\max})$. It is easy to verify that the preceding inequalities hold for $k = 0$ since $\|\tilde{y}(0)\| = 0$ and $V(\zeta(0)) = \tilde{x}_0^\top P \tilde{x}_0$. Assume that these two inequalities hold for k and we show next that they also hold for $k+1$.

Consider $\dot{V}$ over $t \in [kT_s, (k+1)T_s)$. Since $P_o A_o + A_o^\top P_o = -Q_o$, we have

$$\dot{V} = 2\zeta^\top P_o \left(A_o \zeta + \Lambda B \tilde{u} + \Lambda B \sigma \right) \le -\lambda_{\min}(Q_o) \|\zeta\|^2 + 2\|\zeta\| (\|P_o \Lambda B\| \|\tilde{u}\| + \|P_o \Lambda B\| \|\sigma\|).$$

Since $\|x(t)\| \le \rho_x$ for any $t \in [0, t^*)$, we have $\|\sigma(t)\| = \|f(t, x(t))\| \le \sigma_{\max}$ where $\sigma_{\max}$ is defined in (31). Also note that $\|\tilde{u}(t)\| \le \epsilon_{\rm u}$ by (35). Therefore, for any $t \in [kT_s, (k+1)T_s)$

$$\dot{V} \;\le\; -\lambda_{\min}(Q_o) \|\zeta\|^2 + 2\|\zeta\| (\|P_o \Lambda B\| \epsilon_{\rm u} + \|P_o \Lambda B\| \sigma_{\max}) = -\lambda_{\min}(Q_o) \|\zeta\|^2 + a\|\zeta\|.$$

This inequality implies $V(t) \le \alpha$, which means

$$\|\zeta(t)\| \;\le\; \sqrt{\frac{\alpha}{\lambda_{\min}(P_o)}}, \tag{66}$$

$$V((k+1)T_s) \;\le\; \alpha, \tag{67}$$

and therefore $\|\zeta((k+1)T_s)\| \le \sqrt{\frac{\alpha}{\lambda_{\min}(P_o)}}$. Recall that

$$\begin{aligned} \tilde{y}((k+1)T_s) &= (\mathbb{I}, 0) \tilde{\xi}((k+1)T_s) = (\mathbb{I}, 0) \zeta((k+1)T_s) \\ &= (\mathbb{I}, 0) \left(e^{A_o T_s} \begin{pmatrix} y(kT_s) - y_{\rm C}(kT_s) \\ \tilde{y}_\perp(kT_s) \end{pmatrix} + \int_0^{T_s} e^{A_o(T_s - \tau)} \Lambda B (\tilde{u}(\tau) + \sigma(\tau)) d\tau \right). \end{aligned}$$

Let $z = \begin{pmatrix} 0 & (\tilde{y}_\perp(kT_s))^\top \end{pmatrix}^\top \in \mathbb{R}^n$. By the definition of Λ in (14), we have $V(z) \le V(\zeta(kT_s)) \le \alpha$, which implies $\|\tilde{y}_\perp(kT_s)\| \le \sqrt{\frac{\alpha}{\lambda_{\min}(P_o)}}$. Then, with $\|y(kT_s) - y_{\rm C}(kT_s)\| \le \mu$ given by (34), the preceding equation suggests

$$\begin{aligned} \|\tilde{y}((k+1)T_s)\| &\le \|\eta_1(T_s)\| \, \|y(kT_s) - y_{\rm C}(kT_s)\| + \|\eta_2(T_s)\| \|\tilde{y}_\perp(kT_s)\| + \|\eta_3(T_s)\| \, (\epsilon_{\rm u} + \sigma_{\max}) \\ &\le \beta_1(T_s)\mu + \beta_2(T_s) \sqrt{\frac{\alpha}{\lambda_{\min}(P_o)}} + \beta_3(T_s)(\epsilon_{\rm u} + \sigma_{\max}) = \varsigma(T_s, \epsilon_{\rm u}, \mu), \end{aligned}$$

where $\eta_i(T_s)$ and $\beta_i(T_s)$, $i = 1, 2, 3$ are defined in (25), (26), (28). Therefore, we can conclude that for any $k \in \{0, \cdots, k^* - 1\}$, the inequalities $\|\tilde{y}(kT_s)\| \leq \varsigma(T_s, \epsilon_{\rm u}, \mu)$ and $V(\zeta(kT_s)) \leq \alpha$ hold, which completes the mathematical induction. Consequently,

$$\|y_{\rm C}(kT_s) - \hat{y}(kT_s)\| \ \leq \ \|y_{\rm C}(kT_s) - y(kT_s)\| + \|y(kT_s) - \hat{y}(kT_s)\| \ \leq \ \mu + \varsigma(T_s, \epsilon_{\rm u}, \mu). \quad (68)$$

Consider $\|\tilde{y}(t)\|$ over $t \in [kT_s, (k+1)T_s)$ for any $k \in \{0, \cdots, k^* - 1\}$. We know

$$\begin{aligned} & \tilde{y}(t) = (\mathbb{I}, 0)\tilde{\xi}(t) \\ = \ & (\mathbb{I}, 0) \left(e^{A_o(t-kT_s)} \begin{pmatrix} y(kT_s) - \hat{y}(kT_s) \\ \tilde{y}_\perp(kT_s) \end{pmatrix} + \int_{kT_s}^{t} e^{A_o(t-\tau)} \Lambda(B\tilde{u}(\tau) + B\sigma(\tau) - \hat{\sigma}(kT_s)) d\tau \right). \end{aligned}$$

With the adaptation law in (16) and inequality (68), for any $t \in [kT_s, (k+1)T_s)$ and any $k \in \{0, \cdots, k^* - 1\}$, the preceding inequality implies

$$\begin{aligned} \|\tilde{y}(t)\| \ \leq \ & \|\eta_1(t - kT_s)\| \|y(kT_s) - \hat{y}(kT_s)\| + \|\eta_2(t - kT_s)\| \|\tilde{y}_\perp(kT_s)\| \\ & + \|\eta_3(T_s)\| \, \epsilon_{\rm u} + \|\eta_3(T_s)\| \, \sigma_{\max} + \|\eta_4(T_s)\| \, \|y_{\rm C}(kT_s) - \hat{y}(kT_s)\| \\ \leq \ & \beta_1(T_s)\varsigma(T_s, \epsilon_{\rm u}, \mu) + \beta_2(T_s)\sqrt{\tfrac{\alpha}{\lambda_{\min}(P_o)}} + \beta_3(T_s)(\epsilon_{\rm u} + \sigma_{\max}) \\ & + \beta_4(T_s) \left(\mu + \varsigma(T_s, \epsilon_{\rm u}, \mu)\right) \ = \ \theta(T_s, \epsilon_{\rm u}, \mu), \end{aligned}$$

where $\eta_i(T_s)$ and $\beta_i(T_s)$, $i = 1, 2, 3, 4$ are defined in (25), (26), (27), (28). Similarly, we can prove that for any $t \in [k^*T_s, t^*)$, $\|\tilde{y}(t)\| \leq \theta(T_s, \epsilon_{\rm u}, \mu)$ holds. ■

C. Proof of Lemma 5.3

Consider the system in (1) with the continuous-time controller in (11) - (18). Let $\tilde{x} = x - \hat{x}$, $\tilde{u} = u - \hat{v}_{\rm C}$, and $\tilde{y} = C\tilde{x}$. The error dynamics between the system and the state predictor is

$$\dot{\tilde{x}}(t) \ = \ A_m\tilde{x}(t) + B\tilde{u}(t) + B\sigma(t) - \hat{\sigma}(t), \quad (69)$$

where $\sigma(t) = f(t, x(t))$. It implies

$$\tilde{x}(s) = H(s)(B\tilde{u}(s) + B\sigma(s) - \hat{\sigma}(s)) + H(s)\tilde{x}_0 \quad (70)$$

With simple modifications, we can rewrite the preceding equation as

$$\begin{aligned} \hat{C}\tilde{y}(s) \ &= \ H_c(s)\tilde{u}(s) + \frac{H_c(s)}{F(s)}F(s)\sigma(s) - \frac{H_c(s)}{F(s)}H_c(s)^{-1}F(s)\hat{C}CH(s)\hat{\sigma}(s) + \hat{C}CH(s)\tilde{x}_0. \\ &= \ H_c(s)\tilde{u}(s) + \frac{H_c(s)}{F(s)}\left(F(s)\sigma(s) - W(s)\hat{\sigma}(s)\right) + \hat{C}CH(s)\tilde{x}_0. \end{aligned}$$

Recall that $H_c(s) = \hat{C}CH(s)B$ and $W(s) = F(s)H_c(s)^{-1}\hat{C}CH(s)$. It means

$$F(s)\sigma(s) - W(s)\hat{\sigma}(s) \ = \ F(s)H_c(s)^{-1}\hat{C}(\tilde{y}(s) - CH(s)\tilde{x}_0) - F(s)\tilde{u}(s), \quad (71)$$

which, together with (36) and (35) in Lemma 5.2, implies the satisfaction of (40).

Next, consider the real system and the reference system:

$$\begin{aligned} x(s) &= H(s)Bu(s) + H(s)B\sigma(s) + H(s)x_0 \\ &= H(s)Bv_{\rm C}(s) + H(s)B\sigma(s) + H(s)x_0 + H(s)B(u(s) - v_{\rm C}(s)) \\ &= H(s)(BF(s)k_g r(s) + x_0) + H(s)B(\sigma(s) - W(s)\hat{\sigma}(s)) + H(s)B(u(s) - v_{\rm C}(s)), \\ x_{\rm ref}(s) &= H(s)(BF(s)k_g r(s) + \hat{x}_0) + H(s)B(1 - F(s))\sigma_{\rm ref}(s). \end{aligned}$$

With $G(s) = H(s)B(1 - F(s))$, the error dynamic satisfies

$$x(s) - x_{\rm ref}(s) = \underbrace{H(s)B(\sigma(s) - W(s)\hat{\sigma}(s)) - G(s)\sigma_{\rm ref}(s) + H(s)\tilde{x}_0}_{\Psi_1(s)} + \underbrace{H(s)B(u(s) - v_{\rm C}(s))}_{\Psi_2(s)}. \tag{72}$$

Consider $\Psi_1(s)$:

$$\begin{aligned} \Psi_1 &= H(s)B(F(s)\sigma(s) - W(s)\hat{\sigma}(s)) + H(s)B(1 - F(s))\sigma(s) - G(s)\sigma_{\rm ref}(s) + H(s)\tilde{x}_0 \\ &= H(s)B(F(s)\sigma(s) - W(s)\hat{\sigma}(s)) + G(s)\left(\sigma(s) - \sigma_{\rm ref}(s)\right) + H(s)\tilde{x}_0 \\ &= H(s)B\left(F(s)H_c(s)^{-1}\hat{C}\left(\tilde{y}(s) - CH(s)\tilde{x}_0\right) - F(s)\tilde{u}(s)\right) + G(s)\left(\sigma(s) - \sigma_{\rm ref}(s)\right) + H(s)\tilde{x}_0, \end{aligned}$$

where the last equivalence is obtained by applying (71). It means

$$\|\Psi_1(s)\|_{\mathcal{L}_\infty^{[0,t^*]}} \leq b_1\|\tilde{y}\|_{\mathcal{L}_\infty^{[0,t^*]}} + b_2\|\tilde{u}\|_{\mathcal{L}_\infty^{[0,t^*]}} + \|G(s)\|_{\mathcal{L}_1}\|\sigma - \sigma_{\rm ref}\|_{\mathcal{L}_\infty^{[0,t^*]}} + b_3. \tag{73}$$

Consider $\Phi_2(s)$. With $\|\hat{v}_{\rm C}(t) - u(t)\| \leq \epsilon_{\rm u}$ in (35) and the triggering event $\|\hat{v}_{\rm C}(t) - v_{\rm C}(t)\| \leq \epsilon_{\rm u}$, we obtain $\|u(t) - v_{\rm C}(t)\| \leq 2\epsilon_{\rm u}$, which means $\|\Psi_2(s)\|_{\mathcal{L}_\infty^{[0,t^*]}} \leq \epsilon_{\rm u}b_4$. Combining this inequality with (73) yields

$$\begin{aligned} \|x - x_{\rm ref}\|_{\mathcal{L}_\infty^{[0,t^*]}} &\leq \|\Psi_1(s)\|_{\mathcal{L}_\infty^{[0,t^*]}} + \|\Psi_2(s)\|_{\mathcal{L}_\infty^{[0,t^*]}} \\ &\leq b_1\|\tilde{y}\|_{\mathcal{L}_\infty^{[0,t^*]}} + b_2\|\tilde{u}\|_{\mathcal{L}_\infty^{[0,t^*]}} + \|G(s)\|_{\mathcal{L}_1}\|\sigma - \sigma_{\rm ref}\|_{\mathcal{L}_\infty^{[0,t^*]}} + b_3 + \epsilon_{\rm u}b_4. \end{aligned}$$

Since $\|x(t)\| \leq \rho_x$ and $\|x_{\rm ref}(t)\| \leq \rho_x$ hold for any $t \in [0, t^*)$ and $\sigma(t)$, $\sigma_{\rm ref}(t)$ are locally Lipschitz w.r.t. x and $x_{\rm ref}$, respectively, the preceding inequality implies

$$\|x - x_{\rm ref}\|_{\mathcal{L}_\infty^{[0,t^*]}} \leq \frac{b_1\|\tilde{y}\|_{\mathcal{L}_\infty^{[0,t^*]}} + b_2\|\tilde{u}\|_{\mathcal{L}_\infty^{[0,t^*]}} + b_3 + b_4\epsilon_{\rm u}}{1 - \|G(s)\|_{\mathcal{L}_1}L_{\rho_x}} \leq \frac{b_1\theta(T_s, \epsilon_{\rm u}, \mu) + b_2\epsilon_{\rm u} + b_3 + b_4\epsilon_{\rm u}}{1 - \|G(s)\|_{\mathcal{L}_1}L_{\rho_x}},$$

where the last inequality is obtained because of (36) and (35) in Lemma 5.2. ■

D. Proof of Theorem 5.4

We use contradiction method to prove the statement. Suppose that the statement is not true. Then since $x(0)$ and $u(0)$ satisfies $\|x(0) - x_{\rm ref}(0)\| < \gamma_x$ and $\|v_{\rm C}(0) - u_{\rm ref}(0)\| < \gamma_u$, there might be two cases:

Case I: there must exist a time instant $t^* > 0$ such that

$$\|x(t) - x_{\rm ref}(t)\| < \gamma_x, \quad \forall t \in [0, t^*), \tag{74}$$

$$\|x(t^*) - x_{\rm ref}(t^*)\| = \gamma_x, \tag{75}$$

$$\|v_{\rm C}(t) - u_{\rm ref}(t)\| \leq \gamma_u, \quad \forall t \in [0, t^*]. \tag{76}$$

Case II: there must exist a time instant $t^* > 0$ such that

$$\begin{aligned} &\|x(t) - x_{\rm ref}(t)\| \leq \gamma_x, \quad \forall t \in [0, t^*], \\ &\|v_{\rm C}(t) - u_{\rm ref}(t)\| < \gamma_u, \quad \forall t \in [0, t^*), \\ &\|v_{\rm C}(t^*) - u_{\rm ref}(t^*)\| = \gamma_u. \end{aligned} \tag{77}$$

Let us first consider Case I. Inequalities (74) and (76) imply

$$\|x(t)\| < \rho_x = \gamma_x + \rho_{x_{\rm ref}} \quad \text{and} \quad \|u(t)\| \leq \rho_u = \gamma_u + \rho_{u_{\rm ref}}$$

for any $t \in [0, t^*]$. It also means over this time interval $\|f(t, x(t))\| \leq \sigma_{\max} = L_{\rho_x}\rho_x + \rho_0$. Then by Lemma 5.1, we know for any $t \in [0, t^*)$,

$$\|y_{\rm C}(t) - y(t)\| \leq \epsilon_{\rm s} + \bar{\Delta}_{\rm P}\phi(\rho_x, \rho_u) = \mu.$$

Notice that inequality (41) implies the satisfaction of (35) (refer to Remark 5.3). Then we can apply Lemma 5.3 and obtain

$$\|x(t) - x_{\rm ref}(t)\| \leq \frac{b_1\theta(T_s, \epsilon_{\rm u}, \mu) + b_2\epsilon_{\rm u} + b_3 + b_4\epsilon_{\rm u}}{1 - \|G(s)\|_{\mathcal{L}_1}L_{\rho_x}} \tag{78}$$

and therefore $\|x(t^*) - x_{\rm ref}(t^*)\| < \gamma_x$ because of (42). This is contradicted to (75). Therefore, Case I does not hold.

Consider Case II. With the same analysis, we have inequality (78). Consider $\|v_{\rm C} - u_{\rm ref}\|_{\mathcal{L}_\infty^{[0,t^*]}}$.

$$\begin{aligned} \|v_{\rm C} - u_{\rm ref}\|_{\mathcal{L}_\infty^{[0,t^*]}} &= \|F(s)\sigma_{\rm ref}(s) - W(s)\hat{\sigma}(s)\|_{\mathcal{L}_\infty^{[0,t^*]}} \\ &\leq \|F(s)\sigma_{\rm ref}(s) - F(s)\sigma(s)\|_{\mathcal{L}_\infty^{[0,t^*]}} + \|F(s)\sigma(s) - W(s)\hat{\sigma}(s)\|_{\mathcal{L}_\infty^{[0,t^*]}} \\ &\leq \|F(s)\|_{\mathcal{L}_1}L_{\rho_x}\|x - x_{\rm ref}\|_{\mathcal{L}_\infty^{[0,t^*]}} + b_5\theta(T_s, \epsilon_{\rm u}, \mu) + b_6 + \|F(s)\|_{\mathcal{L}_1}\epsilon_{\rm u}, \end{aligned}$$

where the last inequality is obtained by applying (40) in Lemma 5.3. Applying (78) and (42) into the preceding inequality implies $\|v_{\rm C} - u_{\rm ref}\|_{\mathcal{L}_\infty^{[0,t^*]}} < \gamma_u$, which is contradicted to (77). It implies that Case II does not hold either. Therefore, $\|x - x_{\rm ref}\|_{\mathcal{L}_\infty} \leq \gamma_x$ and $\|v_{\rm C} - u_{\rm ref}\|_{\mathcal{L}_\infty} \leq \gamma_u$ hold. Moreover, by Lemma 5.3, inequality (37) holds for $k = 0, 1, \cdots, +\infty$. ■

E. Proof of Corollary 5.5

Without the loss of generality, assume that $t^* \in [\tau_f[k^*], \tau_f[k^*+1])$. Since (A_W, B_W, C_W) and (A_F, B_F, C_F) are the state-space realizations of $W(s)$, $F(s)$, respectively, we can re-write the virtual control input in (18) as $v_{\rm C}(t) = -C_W x_W(t) + C_F x_F(t)$, where $x_W(t)$ and $x_F(t)$ are the states of the filters $W(s)$ and $F(s)$ satisfying

$$\dot{x}_W(t) = A_W x_W(t) + B_W \hat{\sigma}(t), \quad x_W(0) = 0, \tag{79}$$

$$\dot{x}_F(t) = A_F x_F(t) + B_F k_g r(t), \quad x_F(0) = 0. \tag{80}$$

Therefore for any $t \in [\tau_r[i], \tau_f[i+1])$,

$$\begin{aligned} \frac{d}{dt}\|v_{\rm C}(\tau_r[i]) - v_{\rm C}(t)\| &\leq \left\| \frac{d}{dt}(v_{\rm C}(\tau_r[i]) - v_{\rm C}(t)) \right\| = \|C_F \dot{x}_W(t) + C_F \dot{x}_F(t)\| \\ &= \|C_W A_W x_W(t) - C_W B_W \hat{\sigma}(t) + C_F A_F x_F(t) + C_F B_F k_g r(t)\| \\ &\leq \|C_W A_W x_W(t)\| + \|C_W B_W \hat{\sigma}(t)\| + \|C_F A_F x_F(t)\| + \|C_F B_F k_g\| r_{\max}. \end{aligned} \tag{81}$$

By the adaptive law in (16), inequality (37) in Theorem 5.4, and inequality (79), we have

$$\begin{aligned} \|C_W A_W x_W\|_{\mathcal{L}_\infty^{[0,t^*]}} &= \|H_W(s)\hat{\sigma}(s)\|_{\mathcal{L}_\infty^{[0,t^*]}} \\ &\leq \|H_W(s)\Phi(T_s)\|_{\mathcal{L}_1} \|\|\hat{y}(kT_s) - y_{\rm C}(kT_s)\|\| \\ &\leq \|H_W(s)\Phi(T_s)\|_{\mathcal{L}_1} \delta, \end{aligned} \tag{82}$$

where $H_W(s)$ is defined in (50). Also we have

$$\|C_W B_W \hat{\sigma}(t)\| \leq \|C_W B_W \Phi(T_s)\| \|\hat{y}(kT_s) - y_{\rm C}(kT_s)\| \leq \|C_W B_W \Phi(T_s)\| \delta. \tag{83}$$

and $\|C_F A_F x_F(s)\|_{\mathcal{L}_\infty} \leq \|H_F(s)\|_{\mathcal{L}_1} r_{\max}$ from (80), where $H_F(s)$ is defined in (51). Applying this inequality with (83) and (82) into (81) yields

$$\frac{d}{dt}\|v_{\rm C}(\tau_r[i]) - v_{\rm C}(t)\| \leq \psi(\delta, T_s).$$

Solving this differential inequality for any $t \in [\tau_r[i], \tau_f[i+1])$ yields

$$\|v_{\rm C}(\tau_r[i]) - v_{\rm C}(t)\| \leq \psi(\delta, T_s)(t - \tau_r[i]).$$

With $\|v_{\rm C}(\tau_r[i]) - v_{\rm C}(\tau_r[i+1])\| = \epsilon_{\rm u}$, the preceding inequality implies $T_{\rm C}[i] = \tau_r[i+1] - \tau_r[i] \geq \frac{\epsilon_{\rm u}}{\psi(\delta, T_s)}$. Similarly, we can obtain the bound on $T_{\rm P}[i]$. ■

REFERENCES

[1] K. Astrom and B. Wittenmark, *Computer-Controlled Systems: theory and design*, 3rd ed. Prentice-Hall, 1997.

[2] Y. Zheng, D. Owens, and S. Billings, "Fast sampling and stability of nonlinear sampled-data systems: Part 2. sampling rate estimations," *IMA Journal of Mathematical Control and Information*, vol. 7, pp. 13–33, 1990.

[3] D. Nesic, A. Teel, and E. Sontag, "Formulas relating $\mathcal{KL}$ stability estimates of discrete-time and sampled-data nonlinear systems," *Systems and Control Letters*, vol. 38, pp. 49–60, 1999.

[4] G. Walsh, H. Ye, and L. Bushnell, "Stability analysis of networked control systems," *IEEE Transactions on Control Systems Technology*, vol. 10, no. 3, pp. 438–446, 2002.

[5] D. Carnevale, A. R. Teel, and D. Nesic, "Further results on stability of networked control systems: a lyapunov approach," *IEEE Transactions on Automatic Control*, vol. 52, pp. 892–897, 2007.

[6] D. Nesic and A. Teel, "Input-output stability properties of networked control systems," *IEEE Transactions on Automatic Control*, vol. 49, pp. 1650–1667, 2004.

[7] K. Arzen, "A simple event-based PID controller," in *Proceedings of the 14th IFAC World Congress*, 1999.

[8] K. Astrom and B. Bernhardsson, "Comparison of Riemann and Lebesgue sampling for first order stochastic systems," in *Proceedings of IEEE Conference on Decision and Control*, 1999.

[9] P. Tabuada, "Event-Triggered Real-Time Scheduling of Stabilizing Control Tasks," *Automatic Control, IEEE Transactions on*, vol. 52, no. 9, pp. 1680–1685, 2007.

[10] X. Wang and M. Lemmon, "Event-triggering in distributed networked control systems," *IEEE Transactions on Automatic Control*, no. 3, pp. 586–601, 2011.

[11] M. Mazo Jr and P. Tabuada, "On event-triggered and self-triggered control over sensor/actuator networks," in *Proceedings of the 47th Conference on Decision and Control*, 2008.

[12] M. Velasco, P. Marti, and J. Fuertes, "The self triggered task model for real-time control systems," in *Work-in-Progress Session of the 24th IEEE Real-Time Systems Symposium (RTSS03)*, 2003.

[13] M. Lemmon, T. Chantem, X. Hu, and M. Zyskowski, "On self-triggered full information h-infinity controllers," in *Hybrid Systems: computation and control*, 2007.

[14] X. Wang and M. Lemmon, "Self-triggered feedback control systems with finite-gain $\mathcal{L}_2$ stability," *IEEE Transactions on Automatic Control*, vol. 54, no. 3, pp. 452–467, 2009.

[15] A. Anta and P. Tabuada, "To sample or not to sample: Self-triggered control for nonlinear systems," *IEEE Transactions on Automatic Control*, vol. 55, no. 9, pp. 2030–2042, 2010.

[16] H. Yu and P. Antsaklis, "Event-triggered real-time scheduling for stabilization of passive/output feedback passive systems," in *American Control Conference*, 2011, pp. 1674–1679.

[17] M. Donkers and W. Heemels, "Output-based event-triggered control with guaranteed $\mathcal{L}_\infty$-gain and improved event-triggering," in *IEEE Conference on Decision and Control*, 2010.

[18] K. Astrom and B. Wittenmark, *Adaptive control*. Addison-Wesley Longman Publishing Co., Inc. Boston, MA, USA, 1994.

[19] D. Miller and E. Davison, "An adaptive controller which provides an arbitrarily good transientand steady-state response," *IEEE Transactions on Automatic Control*, vol. 36, no. 1, pp. 68–81, 1991.

[20] M. Krstic, P. Kokotovic, and I. Kanellakopoulos, "Transient performance improvement with a new class of adaptive controllers," *Systems and Control Letters*, vol. 21, no. 6, pp. 451–461, 1993.

[21] A. Datta and P. Ioannou, "Performance analysis and improvement in model reference adaptive control," *IEEE Transactions on Automatic Control*, vol. 39, no. 12, pp. 2370–2387, 1994.

[22] G. Bartolini, A. Ferrara, and A. Stotsky, "Robustness and performance of an indirect adaptive control schemein presence of bounded disturbances," *IEEE Transactions on Automatic Control*, vol. 44, no. 4, pp. 789–793, 1999.

[23] N. Hovakimyan and C. Cao, $\mathcal{L}_1$ *Adaptive Control Theory*. Philadelphia, PA: SIAM, 2010.

[24] A. Weinreb and A. B. Jr., "Minimum–time control of a two–link robot arm," *Annual Review in Automatic Programming*, vol. 13, Part 2, no. 0, pp. 195–199, 1985, control Applications of Nonlinear Programming and Optimization.